Published in final edited form as:
Exp Eye Res. 2008 July ; 87(1): 9–21.

Functional characterization of a human aquaporin 0 mutation that leads to a congenital dominant lens cataract

K. Varadaraj[1], **S.S. Kumari**[1], **R. Patil**[2], **M.B. Wax**[2], and **R.T. Mathias**[1]

1 *Physiology and Biophysics, State University of NY, Stony Brook, NY*

2 *Ophthalmology Discovery Research, Alcon Research, Ltd., Fort Worth, TX*

Abstract

The aquaporin (AQP) transmembrane proteins facilitate the movement of water across the plasma membrane. In the lens, AQP0 is expressed in fiber cells and AQP1 in the epithelium. Recently, two individuals were identified with congenital polymorphic autosomal dominant cataracts, due to a single nucleotide base deletion mutation in the lens AQP0. The deletion modified the reading frame resulting in the addition of a premature stop codon. In the present study, we examined the water permeability properties, trafficking and dominant negative effects as well as cytotoxicity due to the mutant AQP0 (Δ213-AQP0) protein. The membrane water permeability (P_w) of Δ213-AQP0 expressing oocytes (14±1 μm/s) was significantly lower than those expressing WT-AQP0 (25±3 μm/s). P_w of water injected control oocytes was 13±2 μm/s. Co-expression of WT-AQP0 with Δ213-AQP0 significantly lowered the P_w (18±3 μm/s) compared to WT-AQP0. With or without the EGFP tag, WT-AQP0 protein localized in the plasma membranes of oocytes and cultured cells whereas Δ213-AQP0 was retained in the ER. Forster Resonance Energy Transfer (FRET) showed that WT-AQP0 partly localized with the co-expressed Δ213-AQP0. Co-localization studies suggest that the mutant AQP0 gained its dominant function by trapping the WT-AQP0 in the ER through hetero-oligomerization. Incubating the cells with chemical chaperones, namely, TMAO and DMSO, did not correct the folding/trafficking defects. Cell death in the Δ213-AQP0 expressing cells was due to necrosis caused by the accumulation of Δ213-AQP0 protein in the ER in cytotoxic proportions. The data show that replacement of the distal end of the 6^{th} TM domain and the C-terminal domain of AQP0 due to the deletion mutation resulted in the impairment of cell membrane P_w, localization of the mutant protein in the ER without trafficking to the plasma membrane, and cytotoxicity due to the accumulation of the mutant protein. Cataracts in patients with this mutation might have resulted from the above mentioned consequences.

Keywords

Aquaporins; Dominant Negative Effect; Membrane Permeability; Cataract; Conformational Diseases; Cytotoxicity

Correspondence to: Kulandaiappan Varadaraj, Department of Physiology and Biophysics, SUNY at Stony Brook, NY 11794-8661, Telephone: 631-444-7551, Fax: 631-444-3432, Email: kvaradaraj@notes.cc.sunysb.edu.

1. Introduction

Lens cataract is a significant problem throughout the world and is responsible for the majority of visual impairment in adult humans. It also accounts for ~30% of blindness in infants. The lens is naturally exposed to physiologically challenging conditions such as lack of blood supply, limited oxidative metabolism and no protein turn-over in the majority of its fiber cells. Any unusual alteration in the membrane proteins necessary for lens homeostasis eventually manifests as a cataract. In humans, cataracts develop due to natural mutations in the lens proteins (congenital cataract) as well as exposure to oxidative agents and natural or man-made radiations (Dovrat and Weinreb, 1999; Spector, 1995).

The ocular lens is a transparent and constantly growing organ with minimum light scattering owing to highly ordered crystallin proteins, intercellular spaces that are smaller than the wavelength of visible light, and terminally differentiated fiber cells that lack organelles, which would absorb and scatter light. Moreover, it is the largest organ in the body that lacks a vasculature, again because blood vessels would scatter and absorb light (Bassnett, 2002; Kinoshita and Merola, 1964; Kinoshita et al., 1981; Trokel, 1962). Lens homeostasis and transparency rely on an internal, self generated circulatory system (reviewed in Mathias et al., 2007).

The AQP family consists of transmembrane channels that allow diffusion of either water exclusively (aquaporins), or water and certain neutral solutes such as glycerol and urea (aquaglyceroporins) across the plasma membrane (Agre, 2005; Agre et al., 2002; Calamita, 2005; Verkman, 2003). In mammals, 13 aquaporins have been identified in various tissues; a recent report documents the expression of aquaporins in stem cells (La Porta et al., 2006). Aquaporins are synthesized as monomers but they assemble into tetramers before being transported to the plasma membrane, even though each monomer functions independently as a water channel (Buck et al., 2007; Manley et al., 2000; Pitonzo and Skach, 2006; Roudier et al., 2002; van Hoek et al., 1995; Verbavatz et al., 1993). Bovine AQP0 cDNA was first cloned by Gorin et al. (1984); however, its function was unclear. The gene structure of human AQP0 was characterized by Pisano and Chepelinsky (1991). Genomic analysis revealed that mammalian AQPs result from gene duplication (Chepelinsky, 1994; Wistow et al., 1991). Delineation of the function of AQP1 as a water channel (Preston et al., 1992) suggested a similar role for the closely related AQP0. *In vitro* (Ball et al., 2003; Chandy et al.,1997; Chepelinsky, 2003; Kushmerick et al.,1995; Mulders et al.,1995; Nemeth-Cahalan and Hall, 2000; Swamy-Mruthinti, 1998; Varadaraj et al., 2005), *in vivo* (Varadaraj et al., 1999) and structural (Harries et al., 2004; Gonen et al., 2005) studies corroborated that AQP0 functions as a water channel. Recent *in vitro* and *in vivo* investigations showed that AQP0 can be regulated by pH and Ca^{2+} (Nemeth-Cahalan and Hall, 2000; Varadaraj et al., 2005).

AQP0 and AQP1 are expressed in the mammalian lens (Hamann et al., 1998; Patil et al., 1997; Varadaraj et al., 2005, 2007); the former is abundant (>50% of the total membrane protein) in the lens fiber cell membranes and the latter is expressed in the anterior and differentiating epithelial cells. AQP1 expression is down-regulated and replaced by AQP0 during fiber cell differentiation (Varadaraj et al., 2007). Lens aquaporins play an important role in the maintenance of the normal flow of water across the epithelial and fiber cells to sustain lens transparency and homeostasis (Mathias et al., 1997, 2007; Varadaraj et al., 2007).

Natural congenital autosomal dominant cataracts due to AQP0 mutations have been reported for humans (Bateman et al., 2000; Berry et al., 2000; Francis et al., 2000a; Geyer et al., 2006) and mice (Cataract Fraser (*Cat*^{Fr}, Shiels and Bassnett, 1996); Cataract lens opacity (*Cat*^{lop}, Shiels and Bassnett, 1996); Cataract Tohoku (*Cat*^{Tohm}, Okamura et al., 2003)).

Knockout of AQP0 in mouse also resulted in cataracts (Shiels et al., 2001). Diabetic conditions result in glycation of AQP0 leading to accelerated lens cataractogenesis (Swamy-Mruthinti, 2001; Swamy-Mruthinti et al., 1999). These data highlight the importance of AQP0 in lens transparency. However, AQP1 deficiency in human (Preston et al., 1994) or mouse (Ma et al., 1998) did not produce any detectable effect on lens transparency. Recently, it has been reported that AQP1 knockout mouse lenses cultured under diabetic conditions showed accelerated cataract development (Ruiz-Ederra and Verkman, 2006).

Aquaporins have two tandem repeats (Fig 1 A,B); each has three transmembrane (TM) α-helices and a hydrophobic loop with conserved asparagine–proline–alanine (NPA) motif. The six TM domains (Fig. 1C; H1–H6) are connected by 5 loops (LA-LE). A highly conserved NPA-motif is present in the loops B and E; the NPA-motif folds into the membrane and form short α-helices (HB and HE) which line the channel pore (de Groot and Grubmuller, 2005; Fu et al., 2000; Gonen et al., 2005; Harries et al., 2004; Jung et al., 1994; Murata et al., 2000; Sui et al., 2001). Biochemical and structural analyses have confirmed that aquaporins are functional only in the tetrameric form in the membrane (Cheng et al., 1997; Murata et al., 2000; Ren et al., 2000; Walz et al., 1997) and that aquaporins that do not form tetramers do not conduct water (Mathai and Agre, 1999).

A single nucleotide base deletion mutation in AQP0 resulted in congenital polymorphic autosomal dominant cataracts in two American individuals of European descent. The deletion mutation at codon 213 in the 6^{th} transmembrane domain created a frameshift which eventually led to the formation of a premature stop codon and shortened the protein to 257 amino acids instead of the 263 amino acids in the wild type (Fig. 1A,B,C; Table 1). The amino acid compositions at the distal end of the 6^{th} transmembrane domain and the C-terminal domain (Bateman et al., 2000; Geyer et al., 2006) were totally altered. Ninety percent of the amino acids at the proximal region of the intracellular C-terminal domain were different compared to the wild type. C-terminal domain amino acids 212-243 which are involved in calcium-calmodulin regulation (Lindsey Rose et al., 2008; Varadaraj et al., 2005) and trafficking of the protein to the plasma membrane (Ball et al., 2003; Varadaraj et al., 2000) changed significantly.

The present study sought to find the cause for the development of cataracts in humans carrying this mutation. To do so, we have used heterologous expression of the mutant AQP0 (Δ213-AQP0) in *Xenopus* oocytes, MDCK and N2A cells. We investigated the water permeability, localization of the Δ213-AQP0 protein and cytotoxicity.

2. Materials and Methods

2.1. Human AQP0 cDNA and expression constructs

Wild type AQP0 (Fig. 1A) coding sequence was amplified by Polymerase Chain Reaction with a set of two appropriate primers for 5′ and 3′ ends (Varadaraj and Skinner, 1994;Varadaraj et al., 1996). Three constructs were made with or without a fluorescent protein (mCherry; a kind gift from Dr. Roger Tsien, UC, San Diego or EGFP) as a tag. We have used pcDNA 3.1 *myc*-His vector (Invitrogen, USA) carrying CMV and T7 promoters for *Xenopus* oocyte and mammalian cell expressions. WT-AQP0 was cloned into pcDNA3.1 *myc*-His vector in between EcoRI and BamHI sites. To facilitate efficient expression, we have introduced a 5′ untranslated region of an amphibian virus-3 gene coding for ICP-18 (Willis et al., 1984) between the T7 promoter and the Kozak sequence. The sequences were confirmed by automated sequencing using fluorescent dye terminators (SUNY at Stony Brook, DNA Sequencing Facility). The fluorescent tag, mCherry or EGFP, was introduced between BamHI and Hind III sites. cRNA was transcribed *in vitro* using T7 RNA polymerase (mMESSAGE mMACHINE kit, Ambion, USA). Purified cRNA was dissolved in distilled water and stored at −80 C until injection into the oocytes. The above mentioned constructs were used for creating the deletion mutation at

amino acid 213 as reported by Geyer et al. (2006; also see Fig 1B). Oligonucleotides were specifically designed to introduce the mutation. QuickChange site-directed mutagenesis kit (Stratagene, USA) was used to incorporate the desired mutation (Kumari et al., 2001). The following sense and antisense primers were used: 5′-CAA TCA TTG GAG GGG TCT GGG CAG CCT C -3′ (sense) and 5′-GAG GCT GCC CAG ACC CCT CCA ATG ATT G -3′ (antisense). Incorporation of the mutation was verified by DNA sequencing.

2.2. cRNA expression in Xenopus oocytes

Mature *Xenopus laevis* female frogs were anesthetized by immersion in 0.1% solution of Tricane (Sigma) in water for 15–30 min; ovarian lobes containing stage V and VI oocytes were removed and defolliculated by incubation in 2 mg/ml collagenase Type II (Sigma) and trypsin inhibitor in Ca^{2+} free oocyte medium for 1hr at room temperature. The oocytes were maintained at 18 C in the oocyte medium supplemented with 100 U/ml penicillin, 0.1 mg/ml streptomycin and 0.1 mg/ml kanamycin or in appropriately diluted L15 medium (Invitrogen, USA) supplemented with 2% heat-inactivated fetal calf serum (Hyclone Laboratories, Inc., UT), 2 mM L-glutamine, 100 U/ml penicillin, 0.1 mg/ml streptomycin and 0.1 mg/ml kanamycin. Except where noted otherwise, oocytes were injected with 25 ng cRNA of the respective construct.

2.3. Oocyte water permeability measurement

Xenopus oocyte membrane water permeability was estimated as described by Varadaraj et al. (1999, 2005) with slight modifications. After cRNA injection, oocytes were incubated for 3 days before the membrane permeability assay was performed. Water permeability (P_w, μm/s) of water injected or cRNA injected *Xenopus* oocytes was estimated from the initial slope of the volume change due to transferring of the oocyte from 180 to 60 mOsm medium at 21°C. Change in the volume of the oocyte was monitored and images were digitized using an Olympus CKX41 inverted fluorescent microscope equipped with a Videoscope Image Intensifier and Ikegami video camera. The video signal was sent to an IBM PC-compatible computer through a Data Translation DT-2851 video frame-grabber board. Images were digitized by the computer every 3 seconds using the software Inspector 6, and oocyte cross-sectional areas were subsequently determined by counting the pixels using Sigma Scan Image Analysis software (Version 5) and the volume was calculated. The oocyte membrane water permeability (P_w) was calculated from the initial change in volume using the equation: $P_w = (dV/dt)/(S_m V_w \Delta c)$, where V (cm^3) is the oocyte volume calculated from the cross-sectional area, S_m (cm2) is the oocyte surface area calculated from the cross-sectional area, V_w is molar volume of water (18 cm^3/mol) and Δc is change in bath osmolarity (0.12×10^{-3} mol/cm^3).

2.4. Immunocytochemistry and western blotting

Oocytes were fixed in 4% paraformaldehyde and 0.2% (v/v) Triton X-100 for 6 h at room temperature, and post-fixation, kept in methanol at 4°C, overnight. After rehydration, the oocytes were fixed with 4% paraformaldehyde and 0.2% (v/v) Triton X-100 in 1X PBS for 24 h, cryosectioned at 12–18 μm thickness using a cryomicrotome (Leica) and stored at −20°C. The sections were blocked with normal goat serum and immunostained with polyclonal rabbit antibody raised against human AQP0 (Chemicon, Alpha Diagnostic International or Abcam, Inc.) or GFP (Santa Cruz, USA) at 1:500 dilution in 5% (w/v) bovine serum albumin in 1X PBS, overnight. After washing, the sections were incubated in fluorescein 5′-isothiocyanate (FITC) conjugated goat anti-rabbit IgG in 1X PBS with 5% bovine serum albumin. The sections were washed in 1X PBS, mounted in anti-fade Vectamount (Vector Labs, USA) containing nuclear stain DAPI and viewed. Optimized Z-sectional digital images were acquired and processed as described (Varadaraj et al., 2007). Figures shown are representative of multiple experiments. Oocyte membrane proteins were used for western blotting to confirm the

expression of the WT-AQP0-mCherry and Δ213-AQP0-EGFP using anti-AQP0 and anti-GFP antibodies, respectively as described (Varadaraj et al., 1997, 2005).

2.5. Cell culture and transfection

Cell culture and transfection were performed as described previously (Kumari et al., 2000) with minor modifications. In short, Madin-Darby Canine Kidney (MDCK) and mouse neuroblastoma (N2A) cells from American Type Culture Collection (Manassas, VA) were grown in Minimum Essential Medium (Invitrogen) supplemented with 10% heat-inactivated fetal calf serum (Hyclone Laboratories, Inc., UT), 1% non-essential amino acids, 2 mM L-glutamine, and 100 U/ml penicillin and 0.1 mg/ml streptomycin. Maintenance of cell cultures was performed at 37°C and 5% CO_2 in a humidified atmosphere. Transfections were carried out using effectene reagent (Qiagen, USA), following the manufacturer's protocol.

2.6. Expression and localization of WT-AQP0-mCherry and Δ213-AQP0-EGFP in cultured mammalian cells

Wild type and mutant AQP0 with mCherry or EGFP tag were transfected separately into MDCK and N2A cells using effectene reagent. For co-localization studies, the constructs were co-transfected. Fluorescent signals were obtained using a Zeiss epifluorescent microscope and mCherry and EGFP fluorescent filters. Forster Resonance Energy Transfer (FRET) was used to examine the co-localization of WT-AQP0 and Δ213-AQP0. We used Δ213-AQP0-EGFP as the donor (Ex 488 and Em 507) and WT-AQP0-mCherry as the acceptor (Ex 587 Em 610). Images were acquired using a Zeiss microscope fitted with a 63X oil immersion lens and equipped with the following filters/dichroic sets (nm): 1. Texas Red cube, excitation (EX) 545/30, emission (EM) 620/60, beamsplitter 570 (longpass); 2. EGFP cube, excitation (EX) 470/40, emission (EM) 525/50, beamsplitter 495 (longpass) and 3. FRET cube, EX 470/40, EM 640/50, beamsplitter 495 (longpass) (Chroma Technology Corp, USA).

To investigate whether the mutant protein localizes in the plasma membrane, Δ213-AQP0-EGFP transfected cells were grown on sterile coverslips, fixed in freshly prepared ice cold 4% paraformaldehyde in 1X PBS for 30 min., washed in cold 1X PBS and incubated with wheat germ agglutinin (WGA; Molecular probes) conjugated to Texas Red-X fluorescent tag (1μg/μl) in a humidified chamber for 30 min. WGA binds to glycosylated proteins, specifically to *N*-acetylglucosamine and *N*-acetyl neuraminic acid (sialic acid) residues. The cells were washed in PBS at room temperature and coverslips were mounted using Vectashield mounting medium (Vector Laboratories, CA) containing nuclear stain DAPI and sealed with clear nail polish. Slides were viewed using an epifluorescent microscope with an excitation band filter of 489 nm and an emission band pass filter of 508 nm for EGFP fluorescence from Δ213-AQP0–EGFP chimeric protein, or an excitation band filter of 595 nm and an emission band pass filter of 615 nm for Texas-Red-X for WGA. Image acquisition and analysis were performed as described in the previous paragraph.

To investigate the localization of mutant AQP0 in the ER, Δ213-AQP0-EGFP transfected cells grown on sterile coverslips were fixed in freshly prepared ice cold 4% paraformaldehyde/0.1% Triton X-100 in 1X PBS for 20 min., washed in cold 1X PBS, blocked with 5% normal donkey serum in 5% BSA and incubated with polyclonal anti-calnexin antibody (calnexin-ER resident protein, Abcam, USA) in 5% BSA, at 4°C overnight in a humidified chamber. The cells were washed at room temperature and incubated with anti-goat IgG (H+L) conjugated to Texas-Red (Santa Cruz, USA). Washing of the slides and subsequent procedures were performed as described for WGA binding.

2.7. Morphological examination of cytotoxicity, necrosis and apoptosis

Necrosis and apoptosis due to the cytotoxicity induced by the Δ213-AQP0 protein in live cells were estimated using Vybrant Apoptosis Assay Kit (Invitrogen) following the protocol provided by the vendor. For the study, MDCK cells were transfected with WT-AQP0 or Δ213-AQP0 cloned into the eukaryotic expression vector pcDNA3.1 *myc*-His without tag as described. For positive controls, cells transfected with only vector were incubated in the culture medium containing 100 μM ebselen or 20 μM camptothecin (Sigma) for 8h at 37°C in the CO_2 incubator to induce necrosis or apoptosis; another group was exposed to 0.1% DMSO (used in dissolving ebselen and camptothecin), in order to find out the solvent effect on necrosis and apoptosis. Two negative controls of cells transfected with only vector were used for comparison. A sham transfected control was also included in the study. All the groups were treated with three nuclear stains, namely, Hoechst 33342, YO-Pro-1 and propidium iodide and observed under Zeiss Axiovert 200 inverted fluorescence microscope using appropriate filters. Live cell nuclei show low level of blue fluorescence, apoptotic cells show bright green and blue fluorescence, and necrotic cells show bright red fluorescence. We counted the total number of WT-AQP0 or Δ213-AQP0 expressing cells (N) and the number of WT-AQP0 or Δ213-AQP0 expressing cells having necrotic or apoptotic nucleus (X) in a selected area. The gross incidence of necrosis or apoptosis in a WT-AQP0 or Δ213-AQP0 transfection was X/N. In each transfection, background occurrence (C) of necrosis or apoptosis was estimated by counting the frequency of only vector transfected cells that showed necrosis or apoptosis. The subtraction, (X/N)–C, represents the specific necrosis or apoptosis. Data presented are the means and SD of four separate transfections.

2.8. Biochemical examination of cytotoxicity using Lactate Dehydrogenase (LDH) assay

MDCK cells were transfected with WT-AQP0 or Δ213-AQP0. In order to reduce background, cells were cultured in the medium without phenol red and containing 2% bovine calf serum. After 72 h, the transfected cells were subjected to the cytotoxicity assay, which compares level of LDH seeped out into the experimental culture medium from the dying cells after membrane breakage due to cytotoxicity, with the LDH level of the healthy cell culture medium. The release of LDH enzyme due to cell lysis was detected using CytoTox 96 Non-radioactive Cytotoxicity Assay (Promega; Cik et al., 1995). In brief, diluted culture medium or cell lysate was added to the substrate mix containing a tetrazolium salt (INT). LDH converts INT into a red formazan product. The intensity of the color formed is proportional to the number of lysed cells. Negative and positive controls were used as described in the previous section. Optical density was measured at 490 nm using a UV-Visible spectrophotometer (Varian Cary Model 100 Bio UV-spectrophotometer). The percentage of cytotoxicity levels was determined by dividing the OD value of the medium in which control or experimental group was cultured (after subtracting the background derived from the medium), by the OD values from the healthy cell lysate supernatant and medium, and multiplying the value by 100.

2.9. 3-D Human AQP0 protein model

A three dimensional model of human wild type AQP0 protein (Fig. 1C) was predicted using 3D-JIGSAW software (Bates et al., 1999,2001;Contreras-Moreira and Bates, 2002) based on the available aquaporin protein models in the Molecular Modeling Database of the Protein Data Bank.

2.10. Statistics

Statistical analyses were performed by student's *t*-test using Sigma Plot 2000 software, Version 6.10. A value of $P < 0.05$ was considered significant.

3. Results

3.1. Functional expression of WT-AQP0 and Δ213-AQP0 proteins

Xenopus oocytes were injected with different concentrations of cRNA for WT-AQP0 to determine the optimal concentration required for obtaining a measurable difference in membrane permeability compared to the water injected oocytes. Membrane water permeability (P_w) of WT-AQP0 cRNA injected oocytes increased in a dose-dependent manner. Fig. 2A shows the P_w of oocytes injected with distilled water (13±2 μm/s), WT-AQP1 (5 ng/oocyte, positive control; 259±59 μm/s), varying concentrations of WT-AQP0 (1, 2, 5, 10, 15, 20, 25, 35, 50 or 75 ng/oocyte), WT-AQP0-mCherry (25 ng/oocyte) or WT-AQP0-EGFP (25ng/oocyte). At a concentration of 25 ng of WT-AQP0 cRNA per oocyte, there was a two fold increase in water permeability (25±3 μm/s) compared to the water injected oocytes (13±2 μm/s); higher concentrations did not show any appreciable increase. With 25 ng cRNA, there was no significant difference in the P_w among WT-AQP0 (25±3 μm/s), WT-AQP0-mCherry (25 ±4 μm/s) and WT-AQP0-EGFP (25±4 μm/s) injected oocytes. Therefore, the optimal concentration of 25 ng cRNA per oocyte was used for further experiments. Reports indicate that AQP1 and the majority of other cloned aquaporins exhibit about 10–40-fold increase in water permeability under different experimental conditions compared to the AQP0 injected oocytes (Chandy et al., 1997;Preston et al., 1992,1993;Zampighi et al., 1995). Our data show ~10 fold increase in Pw of AQP1 (259±59 μm/s) over that of AQP0 (25±3 μm/s; Fig. 2A,B).

P_w of oocytes injected with cRNA for Δ213-AQP0 (14±1 μm/s) or Δ213-AQP0-EGFP (13±1 μm/s) were significantly lower than that of oocytes injected with WT-AQP0 with (25±4 μm/s) or without a fluorescent tag (25±3 μm/s). The P_w of the mutant was the same as that of the water injected control oocytes (13±1 μm/s; Fig. 2C), indicating that the mutation severely interfered with the normal functioning of the protein. In an attempt to correct the folding and/or trafficking defects of the mutant protein, we incubated the oocytes injected with cRNA for Δ213-AQP0-EGFP in the chemical chaperones, Trimethylamine N-oxide (TMAO, 100mM) or DMSO (0.5%) as an additive to the medium, for 48h. The chemical chaperones, however, did not cause any significant increase (Δ213-AQP0-EGFP with TMAO, 16±2 μm/s and Δ213-AQP0-EGFP with DMSO, 15±2 μm/s) in oocyte membrane water permeability (Fig. 2C). We co-injected cRNAs (25 ng each) for WT-AQP0-mCherry and Δ213-AQP0-EGFP. P_w of these oocytes was less (18±3 μm/s) than that of the oocytes injected with only WT-AQP0-mCherry (25±3 μm/s) cRNA (Fig. 2C). Interestingly, co-expression of WT-AQP0 protein did little to improve the water permeability of the Δ213-AQP0 protein. Instead, the Δ213-AQP0 hampered the water permeability of the WT-AQP0, suggesting that the former might have oligomerized with the latter and reduced the number of WT-AQP0 trafficking to the membrane. As for the previous experiment, we tried to correct the misfolding and/or trafficking problems by incubating the co-expressed oocytes in TMAO (100 mM) or DMSO (0.5%) for 48h. The chaperones did not produce any significant improvement (TMAO-treated, 18±4 μm/s and DMSO-treated, 18±3 μm/s) in oocyte membrane water permeability (Fig. 2C).

3.2. Expression and localization of WT-AQP0 and Δ213-AQP0

WT-AQP0 and Δ213-AQP0 proteins with fluorescent tags, mCherry and EGFP, were separately expressed in *Xenopus* oocytes, viewed under an epifluorescent microscope and images were digitized (Fig. 3). Water injected oocytes are shown in Fig. 3A and C (mild autofluorescence is seen). The red oocyte in Fig. 3B was injected with cRNA for WT-AQP0-mCherry and the green oocyte in Fig. 3D, with Δ213-AQP0-EGFP; the orange oocytes in Fig. 3E and F were images, taken using filters for mCherry and EGFP, of oocytes co-injected with both cRNAs and merged with each other. These images mainly demonstrate the expression of WT-AQP0-mCherry and Δ213-AQP0-EGFP cRNAs injected either separately or together into the oocytes. Tag fluorescence aided in the initial screening of oocytes and cells expressing

WT-AQP0-mCherry and/or mutant AQP0-EGFP cRNAs for conducting water permeability, co-localization and FRET studies.

Oocytes expressing WT-AQP0 were cryosectioned and immunostained using anti-AQP0 antibody. Localization of Δ213-AQP0-EGFP was determined from EGFP fluorescence. Fig. 3G-M shows localization of WT-AQP0-mCherry and Δ213-AQP0-EGFP proteins. Confocal fluorescence microscopy showed no immunostaining in water injected oocytes (Fig. 3G), significant localization of WT-AQP0 in the oocyte plasma membrane (Fig. 3H–J), very little, if any, Δ213-AQP0-EGFP in the plasma membrane (Fig. 3K–M). Chaperone-treated oocytes expressing WT (Fig. 3I,J) or mutant (Fig. 3L,M) AQP0 showed no significant difference in the pattern of expression compared to their respective untreated oocytes. Fig. 3N shows immunostaining of WT-AQP0 when co-expressed with Δ213-AQP0 without EGFP tag. There appears to be some staining of the plasma membrane, but most of the protein has localized in the subcellular compartments (yellow arrows).

Immunoblot analysis of total membrane extracts from oocytes injected with WT-AQP0-mCherry, Δ213-AQP0-EGFP or co-injected with cRNAs of both constructs confirmed the expression of the respective protein with an expected peptide band size of ~58 kDa (AQP0, ~28 kDa plus mCherry or EGFP, ~30 kDa; Fig. 3O). Protein expression levels of the oocytes quantified by densitometry (data not shown) showed no significant difference between WT-AQP0-mCherry and Δ213-AQP0-EGFP as revealed by the western blot (Fig. 3O, lanes 1 and 2). Similarly, there was no significant difference in WT-AQP0-mCherry protein expression when injected singly or combined with the Δ213-AQP0-EGFP (Fig. 3O, lanes 3 and 4). Therefore, reduction in the water permeability of the co-expressed oocytes cannot be attributed to the difference in the expression levels of the wild type protein.

WT-AQP0-mCherry and Δ213-AQP0-EGFP were transfected separately or together into MDCK cells (Fig. 4). As noticed for the oocytes in Fig. 3, WT-AQP0-mCherry chimeric protein localized abundantly in the plasma membrane (Fig. 4A) whereas Δ213-AQP0-EGFP localized predominantly in the cytoplasmic compartments (Fig. 4B,C,E). XZ-axis confocal images (just below each image) clearly reveal the difference in WT-AQP0-mCherry (Fig. 4A) and Δ213-AQP0-EGFP (Fig. 4B) protein localization, in the plasma membrane and cytoplasmic organelles, respectively. Cells expressing Δ213-AQP0-EGFP (Fig. 4C) were stained with wheat germ agglutinin conjugated to Texas Red-X (WGA-Texas Red-X) which showed plasma membrane specific binding (Fig. 4D) of glycosylated proteins. However, fluorescence from Δ213-AQP0-EGFP and WGA-Texas Red-X did not show any sign of co-localization (Fig. 4E). When WT-AQP0-mCherry and Δ213-AQP0-EGFP were co-expressed, both chimeric proteins showed signal in the cytoplasmic compartments (Fig. 4F,G). Merger of WT-AQP0-mCherry and Δ213-AQP0-EGFP images taken from the same cell showed co-localization of the WT and mutant proteins (Fig. 4H); co-localization in the cytoplasmic organelles is more noticeable in the XZ-axis merged confocal image below 4H.

To determine if WT-AQP0-mCherry and Δ213-AQP0-EGFP oligomerize and co-localize in the ER, we transfected these constructs into N2A or MDCK cells either individually to check the background or together for FRET analysis. EGFP served as donor fluorophore and mCherry as acceptor for FRET. Cells transfected with WT-AQP0-mCherry or Δ213-AQP0-EGFP showed red (Fig. 5A) or green (Fig. 5E) fluorescence of the respective tags, but showed very low background signal in other fluorescent filters (Fig. 5B,D) or in FRET filter (Fig. 5C,F). Fig. 5G-I shows images of a cell that co-expressed WT-AQP0-mCherry and Δ213-AQP0-EGFP. The fluorescence of WT-AQP0-mCherry is shown in Fig. 5G and that of Δ213-AQP0-EGFP in Fig. 5H. Fig. 5I shows the FRET signal, suggesting the localization of wild type and mutant proteins in the same oligomers or within 100Å. To determine if Δ213-AQP0-EGFP is localized in the ER without trafficking to the plasma membrane, we transfected MDCK cells

with Δ213-AQP0-EGFP. Two days post-transfection, the cells were fixed and immunostained with anti-calnexin antibody. Calnexin is an ER resident protein. Fig. 6A shows the expression of Δ213-AQP0-EGFP chimeric protein and Fig. 6B shows anti-calnexin antibody binding. Fig. 6C is the overlaid image; the orange color suggests colocalization of both proteins in the ER.

3.3. Effect of the mutant AQP0 on cell viability

Aberrant protein accumulation in tissues and cellular compartments leads to several disorders in humans called conformational diseases. Accumulation of misfolded proteins in the ER causes ER stress that ultimately leads to cell death. Our immunocytochemical and colocalization studies showed that Δ213-AQP0 localized in the ER and also trapped the WT-AQP0 when expressed together. Therefore, accumulation of the mutant transmembrane protein alone or along with the wild type in the ER could induce lens fiber cell death and cause congenital lens cataract. To test this hypothesis, we asked: Can heterologous expression of Δ213-AQP0 induce cell death? If so, does it happen by necrosis or by apoptosis? For answers, we transfected WT-AQP0 and Δ213-AQP0 in MDCK cells and performed morphological and biochemical assays to evaluate cytotoxicity due to mutant protein accumulation in the ER.

Morphological studies using The Vybrant Apoptosis Assay Kit 7 showed that nuclei of the majority of negative control live cells did not take up propidium iodide stain (bright red) specific for necrosis, or Hoechst 33342 stain (bright blue) specific for apoptosis (Fig. 7A, top three rows); the cells maintained their normal morphology with typical cuboidal shape and a large nucleus (Fig. 7B, a). The positive control cells subjected to necrosis by ebselen treatment showed significant numbers of plasma membrane compromised necrotic cell nuclei which took up propidium iodide stain (Fig. 7A; B, c,d). The necrotic cells showed considerably altered cellular morphology; cells were round, contained large vacuoles and developed perforations in the plasma membrane (Fig. 7B, c,d). Camptothecin induced positive control apoptotic cells showed intense staining for both Hoechst 33342 (bright blue) (Fig. 7A) and YO-Pro-1 (bright green, data not shown) and exhibited fragmented nuclei. On the other hand, cells expressing WT-AQP0 showed no significant difference in the number of necrotic or apoptotic cells compared to the negative controls (Fig. 7A,C). However, Δ213-AQP0 expressing cells showed ~3-fold increase in the amount of necrotic cells (Fig. 7A,C) compared to the wild type, with morphology as seen in ebselen induced positive control necrotic cells (Fig. 7B, e,f); similarly, co-expressed WT-AQP0 and 213-AQP0 cells also showed higher incidence of necrosis. An example of the co-expressed cell showing necrosis is shown in Fig. 7B, g–i.

To further confirm the result that the expression of Δ213-AQP0 protein induced cell death by necrosis and through the loss of cell membrane integrity, a more specific assay that determines the extracellular release of LDH protein (a specific marker for necrosis) into the medium, was employed. LDH is a stable cytosolic enzyme that is released into the extracellular medium upon cell lysis. LDH activity in the mutant transfected cells after 72 hours was ~3 times that of the WT-AQP0 transfected cells and negative controls (Fig. 7D). The LDH leakage corroborated the loss of plasma membrane integrity and was consistent with the morphological data shown in Fig. 7B. These results support the hypothesis that Δ213-AQP0 protein accumulation causes ER stress and contributes to the development of human congenital lens cataract.

4. Discussion

The evidence presented here suggests that the Δ213-AQP0 water channel is nonfunctional due to its failure to properly traffic to the plasma membrane. Under normal conditions, aquaporins are synthesized as monomers, folded and tetramerized as quaternary structural units in the ER before being transported for insertion into the plasma membrane (Buck et al., 2007; Duchesne, et al., 2002; Manley et al., 2000; Pitonzo and Skach, 2006; Roudier et al., 2002; van Hoek et

al., 1995; Verbavatz et al., 1993). The lack of membrane water permeability in oocytes expressing the Δ213-AQP0 might be due to the absence of functional AQP0 in the plasma membrane rather than the level of protein expression. Misfolding and protein trapping in the ER have been reported for several mutant membrane proteins (Denning et al., 1992; Kaushal and Khorana, 1994; Tamarappoo and Verkman, 1998). Our co-expression studies revealed that the Δ213-AQP0 interfered with the normal function of WT-AQP0. Presumably, the Δ213-AQP0 assembles with the WT-AQP0 during oligomerization and retains the wild type also in the ER. This type of oligomerization reduces the number of available WT-AQP0 in the plasma membrane for water permeability and might have led to the development of congenital dominant lens cataract in the two individuals with this mutation.

Several of the naturally occurring AQP0 point mutations that result in lens cataract have been functionally characterized. In human AQP0, E134G and T138R mutations resulted in loss of water permeability due to the failure in trafficking of the proteins to the plasma membrane. However, when the E134G or T138R mutant was co-expressed with WT-AQP0 protein, the mutant protein reached the plasma membrane but caused instability of the tetramers and loss of function in the wild-type AQP0 (Francis et al., 2000b; Harris et al., 2004). Mistargeting of mutant AQP0 to ER-like compartments has previously been reported for mutant mouse models such as *Cat*^{Fr} and *Cat*^{lop} (Shiels and Bassnett, 1996; Shiels et al., 2000). Based on the intense AQP0 immunostaining in the fiber cell membrane of the *Cat*$^{Fr/+}$, Shiels et al. (2000) suggested that in the heterozygous *Cat*$^{Fr/+}$ lens, the mutant AQP0 did not inhibit targeting of the wild type AQP0 to the plasma membrane. *Cat*^{Fr} mutation is caused by truncation and mis-splicing of the long terminal repeat (LTR) sequence of an early transposon (*Etn*) element (Shiels and Bassnett, 1996). This mutation resulted in the expression of a chimeric protein consisting of ~75% AQP0 and ~25% *Etn* LTR amino acid sequence. The predicted LTR amino acid sequence (203–261) replaced most of the 6th transmembrane domain and the entire C-terminal domain of wild-type AQP0 (203–263) with 55 variations, which include calcium-calmodulin binding site and several phosphorylation sites. Human Δ213-AQP0 (Fig. 1; Table 1) is similar to C*at*^{Fr} mutation; in both cases, the 6th TM and C-terminal domains are altered. However, severity of the cataract is more pronounced in lens expressing *Cat*^{Fr} than Δ213-AQP0 protein. This may be due to the difference in species, degree of 6th TM domain deletion, composition of the newly added amino acids or presence of the transposon (*Etn*) element, or due to two or more of these aspects acting in combination.

Trafficking problems associated with mutant AQP2 had been rescued by incubating the cells expressing the mutant protein in chemical chaperones such as glycerol, TMAO or DMSO (Tamarappoo and Verkman, 1998; Shepshelovich et al., 2005). We incubated *Xenopus* oocytes expressing Δ213-AQP0 and/or WT-AQP0 in TMAO or DMSO (Fig. 2), but the folding and/or trafficking problem(s) persisted. Moreover, several disease-associated mutant proteins have shown temperature sensitivity during initial conformation, synthesis or transportation of the cargo to the final destination. These proteins reached the target when incubated at reduced temperatures (Denning et al., 1992). During the course of the Δ213-AQP0 experiments, *Xenopus* oocytes were incubated at 18°C, which should have been low enough to deter simple conformational or folding defects, but it did not. The transport of synthesized and folded proteins to their final destination involves a series of steps, which are directed by the signaling elements present in the amino acid sequence of the cargo protein. Our studies have suggested that the proximal region of the C-terminal containing amino acids 223 to 234 in the WT-AQP0 is critical and may carry sorting signal(s) for targeting of the protein to plasma membrane (Varadaraj et al., 2000). The frameshift in Δ213-AQP0 resulted in 90% of the amino acids being different at the proximal region of the intracellular C-terminal domain (Fig. 1; Table 1). This may be a reason for the trafficking problems.

Previous *in vivo* and *in vitro* studies of AQP0 mutant proteins showed ER localization irrespective of the site of the mutation. In *Cat*^{Fr} mouse, 6th TM and C-terminal domains replaced by the transposon (*Etn*) element resulted in ER localization (Shiels and Bassnett, 1996; Shiels et al., 2000). In the *Cat*^{lop} mouse model, a missense mutation (A51P) in the 2nd transmembrane domain impaired trafficking and retained the mutated AQP0 protein in the ER (Shiels and Bassnett, 1996). In *Hfi* mutant mouse, deletion of 55 amino acids in the 4th and 5th TM interfered with the trafficking of the mutated AQP0 protein to the plasma membrane (Sidjanin, et al., 2001). Deletion of the proximal end of the C-terminal domain of human (Ball et al., 2003; Varadaraj et al., 2000), bovine and mouse (our unpublished data) AQP0s resulted in ER localization. In chimeric protein studies involving AQP0 and AQP2, loop B or C of AQP2 caused the chimeric protein to remain in the ER (Kuwahara et al., 1999). In view of these findings, perhaps mutation in the C-terminal or other domains of AQP0 caused the mutant protein to localize in the ER. Loss of the C-terminal domain or mutation(s) in this region could cause elimination of trafficking signals, alteration in folding and/or prevention of calcium-calmodulin interactions (Lindsey et al., 2008; Varadaraj et al., 2000, 2005). Localization of Δ213-AQP0 in the ER could be due to the following, singly or in combination: 1. Alteration in protein folding influenced by the frameshift which changed the amino acid sequences of the distal end of the 6th TM domain and the C-terminal domain, 2. Loss of the original C-terminal end which carries signals for trafficking and calcium-calmodulin interaction, and 3. Presence of the newly introduced amino acid sequences of the mutated C-terminal domain resulting from the frameshift.

All AQP2 missense mutations in the transmembrane domain and channel forming regions documented so far result in misfolding and trapping of the proteins in the ER and cause recessive nephrogenic diabetes insipidus (NDI). When mutant AQP2 was co-expressed with the WT they did not form heterotetramers due to failure of interaction between the mutant and wild type (Deen et al., 1994; Kamsteeg et al., 1999; Robben et al., 2006). Conversely, mutations in AQP2 C-terminal domain, which carries sorting signal(s), mostly result in dominant NDI because the mutant protein forms heterotetramers allowing only a low level of functional wild type AQP2 in the plasma membrane (de Mattia et al., 2004; Kamsteeg et al., 1999; Kuwahara et al., 2001; Marr et al., 2002). Similarly, in the present investigation, when WT-AQP0 and Δ213-AQP0 were co-expressed, they appeared to form hetero-oligomers in the ER and did not traffic to the plasma membrane.

ER is a multifunctional signaling organelle that controls a wide range of cellular processes including protein folding, trafficking and cellular responses to stress (Liu and Kaufman, 2003). Mutations which do not affect either expression or function but result in conformational instability cause the affected protein to unfold and undergo intermolecular linkage and aggregation, triggering ER stress or unfolded protein response (Carrell, 2005; Carrell and Lomas, 2002; Harding et al., 2002; Lomas and Carrell, 2002). If the ER stress is severe or prolonged, ER-associated cytotoxic cell death pathways are activated (Harding et al., 2002). The aggregation of conformationally destabilized proteins is responsible for more than 20 diseases (reviewed in Stefani and Dobson, 2003) including lens cataract (Crabbel, 1998; Kosinski-Collins and King, 2003; Sandilands, et al., 2002). The majority of congenital and senile cataracts are associated with conformational changes and unfolding of proteins in the lens (Kosinski-Collins and King, 2003; Sandilands, et al., 2002). In the human AQP0 mutation studied here, lens fiber cell damage is mostly in the inner cortex and nucleus (Geyer et al., 2006), where mature fiber cells are devoid of cell organelles, especially ER which normally deals with the mutant proteins through the ER stress response mechanism. More than 50% of the membrane protein in the lens is contributed by AQP0. In the absence of ER in the mature fiber cells, the main defense is α-crystallin chaperone proteins (Das and Surewicz, 1995; Horwitz, 1992; Jakob et al., 1994; Raman and Rao, 1994), which seem insufficient to counteract

the cytotoxicity induced by the mutant AQP0. This situation apparently leads to fiber cell necrosis and cortical and nuclear lens cataract development.

When the cells are exposed to traumatic events such as hypothermia, hypoxia or cytotoxicity due to deleterious mutations that encode toxic proteins, passive cell swelling and injury to cytoplasmic organelles occur leading to membrane lysis, release of cellular contents, and inflammation, all of which contribute to necrosis (Kerr, 1991; Schwartz et al., 1993). In contrast, apoptosis is a mode of cell death that occurs under normal physiological conditions such as normal cell turnover and maintenance of tissue homeostasis and the cell is an active participant. It is an active physiological process of cell damage with specific morphological and molecular characteristics such as cell shrinkage, membrane blebbing, nuclear pyknosis, chromatin condensation and genomic DNA fragmentation (Bursch et al., 1992; Kerr et al., 1972). Leakage of cellular contents by necrotic cells causes a proinflammatory response in the neighboring cells whereas in apoptotic cells, the cellular contents remain within the dying cells and do not affect the neighboring cells (Bonfoco et al., 1995). Under normal physiological conditions, damage in the lens fiber cell plasma membrane of patients having this mutation could be the outcome of cytotoxicity induced by the accumulated Δ213-AQP0 protein and the inadequacy of functional AQP0 water channel in the membrane to regulate cell volume in order to maintain homeostasis. The lenses of patients with this mutation showed punctate cortical opacities and vacuoles in the lens nucleus. This lens phenotype is very similar to that observed in AQP0 mutant mouse models. Lens fiber cells of AQP0 mutant mice exhibited swelling and membrane breakage (Okamura et al., 2003; Shiels et al., 2000, 2001; Shiels and Bassnett, 1996; Sidjanin et al., 2001) as noticed for the MDCK cells expressing Δ213-AQP0 (Fig. 7B). Necrosis is the result when impairment of the cell's ability to maintain homeostasis leads to an influx of extracellular ions followed by water causing cell swelling and eventual rupture. It has been shown experimentally that aquaporins play a critical role in lens transparency and homeostasis (Varadaraj et al., 1999, 2005, 2007), and, knockout of mAQP0 also caused cataract (Al-Ghoul et al., 2003; Shiels et al., 2001). Mature fiber cells in the lens are terminally differentiated and cannot undergo apoptosis due to the lack of functional apoptotic pathway components. When lens fiber cells are exposed to traumatic events, necrosis and cataracts occur.

In conclusion, this investigation suggests the involvement of the 6th TM and C-terminal domains in AQP0 protein trafficking. Replacement of the amino acids in these domains due to the frameshift might have altered the protein trafficking signal(s) or conformation and hampered the normal trafficking and functioning of the protein. Further studies to pinpoint the critical amino acid(s) in this domain responsible for normal trafficking and localization of the protein in the plasma membrane are in progress. Development of lens cataract due to this deletion mutation could be the effects of the following: 1) loss of water permeability, 2) gain of function of trapping the wild type AQP0 in the ER by hetero-oligomerization, thus preventing the WT-AQP0 protein from trafficking to the plasma membrane, and 3) cytotoxicity due to the accumulation of membrane protein in the fiber cells. Better understanding of the inherited cataract development mechanisms due to mutated lens proteins will help to develop chemical chaperones to correct the folding and/or trafficking problems in patients with heritable lens cataract.

Acknowledgements

This work was supported by Alcon Research Ltd., Grant number: 39733; National Institute of Health, Grant number: EY06391.

The abbreviations used are

AQP

Aquaporin

MIP

Major Intrinsic Protein of Lens

FRET

Forster Resonance Energy Transfer

N2A

Neruroblastoma cell line

MDCK

Madin-Darby Canine Kidney

P_w

Membrane water permeability

WGA

Wheat Germ Agglutinin

References

Agre P. Membrane water transport and aquaporins: looking back. Biol Cell 2005;97:355–356. [PubMed: 15901244]

Agre P, King LS, Yasui M, Guggino WB, Ottersen OP, Fujiyoshi Y, Engel A, Nielsen S. Aquaporin water channels - from atomic structure to clinical medicine. J Physiol 2002;542:3–16. [PubMed: 12096044]

Al-Ghoul KJ, Kirk T, Kuszak AJ, Zoltoski RK, Shiels A, Kuszak JR. Lens structure in MIP-deficient mice. Anat Rec A Discov Mol Cell Evol Biol 2003;273:714–730. [PubMed: 12845708]

Ball LE, Little M, Nowak MW, Garland DL, Crouch RK, Schey KL. Water permeability of C-terminally truncated aquaporin 0 (AQP0 1-243) observed in the aging human lens. Invest Ophthalmol Vis Sci 2003;44:4820–4828. [PubMed: 14578404]

Bateman JB, Johannes M, Flodman P, Geyer DD, Clancy KP, Heinzmann C, Kojis T, Berry R, Sparkes RS, Spence MA. A new locus for autosomal dominant cataract on chromosome 12q13. Invest Ophthalmol Vis Sci 2000;41:2665–2670. [PubMed: 10937580]

Bates PA, Sternberg MJE. Model building by comparison at casp3: using expert knowledge and computer automation. Proteins: Structure, Function and Genetics 1999;(Suppl 3):47–54.

Bates PA, Kelley LA, MacCallum RM, Sternberg MJE. Enhancement of protein modelling by human intervention in applying the automatic programs 3D-JIGSAW and 3D-PSSM. Proteins: Structure, Function and Genetics 2001;(Suppl 5):39–46.

Bassnett S. Lens organelle degradation. Exp Eye Res 2002;74:1–6. [PubMed: 11878813]

Berry V, Francis P, Kaushal S, Moore A, Bhattacharya S. Missense mutations in MIP underlie autosomal dominant ‘polymorphic’ and lamellar cataracts linked to 12q. Nat Genet 2000;25:15–17. [PubMed: 10802646]

Bonfoco E, Krainc D, Ankarcrona M, Nicotera P, Lipton SA. Apoptosis and necrosis: Two distinct events induced, respectively, by mild and intense insults with N-methyl-D-aspartate or nitric oxide/superoxide in cortical cell cultures. Proc Natl Acad Sci USA 1995;92:7162–7166. [PubMed: 7638161]

Buck TM, Wagner J, Grund S, Skach WR. A novel tripartite motif involved in aquaporin topogenesis, monomer folding and tetramerization. Nature Struct Mol Biol 2007;14:762–769. [PubMed: 17632520]

Bursch W, Oberhammer F, Schulte-Hermann R. Cell death by apoptosis and its protective role against disease. Trends Pharmacol Sci 1992;13:245–251. [PubMed: 1631963]

Calamita G. Aquaporins: highways for cells to recycle water with the outside world. Biol Cell 2005;97:351–353. [PubMed: 15901243]

Carrell RW. Cell toxicity and conformational disease. Trends Cell Biol 2005;15:574–580. [PubMed: 16202603]

Carrell RW, Lomas DA. Alpha1-antitrypsin deficiency: a model for conformational diseases. N Engl J Med 2002;346:45–53. [PubMed: 11778003]

Chandy G, Zampighi GA, Kreman M, Hall JE. Comparison of the water transporting properties of MIP and AQP1. J Membr Biol 1997;159:29–39. [PubMed: 9309208]

Cheng A, van Hoek AN, Yeager M, Verkman AS, Mitra AK. Three-dimensional organization of a human water channel. Nature 1997;387:627–630. [PubMed: 9177354]

Chepelinsky, AB. The MIP Transmembrane Channel Gene Family. In: Peracchia, C., editor. Handbook of Membrane Channels. Academic Press; New York, USA: 1994. p. 413-432.

Chepelinsky AB. The ocular lens fiber membrane specific protein MIP/aquaporin. J Exp Zool 2003;300A: 41–46.

Cik M, Chazot PL, Coleman SK, Stephenson FA. Using Promega's CytoTox 96® Non-Radioactive Cytotoxicity Assay to measure cell death mediated by NMDA receptor subunits. Promega Notes 1995;51:21.22.

Contreras-Moreira B, Bates PA. Domain Fishing: a first step in protein comparative modelling. Bioinformatics 2002;18:1141–1142. [PubMed: 12176841]

Crabbe MJ. Cataract as a conformational disease--the Maillard reaction, alpha-crystallin and chemotherapy. Cell Mol Biol Noisy-le-grand 1998;44:1047–1050. [PubMed: 9846886]

Das KP, Surewicz WK. On the substrate specificity of alpha-crystallin as a molecular chaperone. Biochem J 1995;311:367–370. [PubMed: 7487869]

de Mattia F, Savelkoul PJ, Bichet DG, Kamsteeg EJ, Konings IB, Marr N, Arthus MF, Lonergan M, van Os CH, van der Sluijs P, Robertson G, Deen PM. A novel mechanism in recessive nephrogenic diabetes insipidus: wild-type aquaporin-2 rescues the apical membrane expression of intracellularly retained AQP2-P262L. Hum Mol Genet 2004;13:3045–3056. [PubMed: 15509592]

de Groot BL, Grubmuller H. The dynamics and energetics of water permeation and proton exclusion in aquaporins. Curr Opin Struct Biol 2005;15:176–183. [PubMed: 15837176]

Deen PMT, Verdijk MAJ, Knoers NVAM, Wieringa B, Monnens LAH, van Os CH, van Oost BA. Requirement of human renal water channel aquaporin-2 for vasopressindependent concentration of urine. Science 1994;264:92–95. [PubMed: 8140421]

Denning GM, Anderson MP, Amara JF, Marshall J, Smith AE, Michael J, Welsh MJ. Processing of mutant cystic fibrosis transmembrane conductance regulator is temperature-sensitive. Nature 1992;358:761–764. [PubMed: 1380673]

Dovrat A, Weinreb O. Effects of UV-A radiation on lens epithelial Na K-ATPase in organ culture. Invest Ophthalmol Vis Sci 1999;40:1616–1620. [PubMed: 10359347]

Duchesne L, Pellerin I, Delamarche C, Deschamps S, Lagree V, Froger A, Bonnec G, Thomas D, Hubert JF. Role of C-terminal domain and transmembrane helices 5 and 6 in function and quaternary structure of major intrinsic proteins: analysis of aquaporin/glycerol facilitator chimeric proteins. J Biol Chem 2002;277:20598–20604. [PubMed: 11927589]

Francis P, Berry V, Bhattacharya S, Moore A. Congenital progressive polymorphic cataract caused by a mutation in the major intrinsic protein of the lens, MIP AQP0. Br J Ophthalmol 2000a;84:1376–1379. [PubMed: 11090476]

Francis P, Chung JJ, Yasui M, Berry V, Moore A, Wyatt MK, Wistow G, Bhattacharya SS, Agre P. Functional impairment of lens aquaporin in two families with dominantly inherited cataracts. Hum Mol Genet 2000b;9:2329–2334. [PubMed: 11001937]

Fu D, Libson A, Miercke LJ, Weitzman C, Nollert P, Krucinski J, Stroud RM. Structure of a glycerol-conducting channel and the basis for its selectivity. Science 2000;290:481–486. [PubMed: 11039922]

Geyer DD, Spence MA, Johannes M, Flodman P, Clancy KP, Berry R, Sparkes RS, Jonsen MD, Isenberg SJ, Bateman JB. Novel single-base deletional mutation in major intrinsic protein MIP in autosomal dominant cataract. Am J Ophthalmol 2006;141:761–763. [PubMed: 16564824]

Gonen T, Cheng Y, Sliz P, Hiroaki Y, Fujiyoshi Y, Harrison SC, Walz T. Lipid–protein interactions in double-layered two-dimensional AQP0 crystals. Nature 2005;438:633–638. [PubMed: 16319884]

Gorin MB, Yancey SB, Cline J, Revel JP, Horwitz J. The major intrinsic protein MIP of the bovine lens fiber membrane: characterization and structure based on cDNA cloning. Cell 1984;39:49–59. [PubMed: 6207938]

Hamann S, Zeuthen T, La Cour M, Ottersen OP, Agre P, Nielsen S. Aquaporins in complex tissues: distribution of aquaporins 1–5 in human and rat eye. Am J Physiol 1998;274:C1332–C1345. [PubMed: 9612221]

Harding HP, Calfon M, Urano F, Novoa I, Ron D. Transcriptional and translational control in the Mammalian unfolded protein response. Annu Rev Cell Dev Biol 2002;18:575–599. [PubMed: 12142265]

Harries WE, Akhavan D, Miercke LJ, Khademi S, Stroud RM. The channel architecture of aquaporin 0 at a 2.2-Å resolution. Proc Natl Acad Sci USA 2004;101:14045–14050. [PubMed: 15377788]

Horwitz J. Alpha-crystallin can function as a molecular chaperone. Proc Natl Acad Sci USA 1992;89:10449–10453. [PubMed: 1438232]

Jakob U, Gaestel M, Engel M, Buchner J. Small heat shock proteins are molecular chaperones. J Biol Chem 1993;268:1517–1520. [PubMed: 8093612]

Jung JS, Preston GM, Smith BL, Guggino WB, Agre P. Molecular structure of the water channel through aquaporin CHIP: the hourglass model. J Biol Chem 1994;269:14648–14654. [PubMed: 7514176]

Kamsteeg EJ, Wormhoudt TA, Rijss JPL, van Os CH, Deen PMT. An impaired routing of wild-type aquaporin-2 after tetramerization with an aquaporin-2 mutant explains dominant nephrogenic diabetes insipidus. EMBO J 1999;18:2394–2400. [PubMed: 10228154]

Kaushal S, Khorana HG. Structure and function in rhodopsin. 7. Point mutations associated with autosomal dominant retinitis pigmentosa. Biochemistry 1994;33:6121–6128. [PubMed: 8193125]

Kerr, JFR. Apoptosis: The Molecular Basis of Cell Death: Current Communications on Cell and Molecular Biology. 3. Cold Spring Harbor Lab. Press; Plainview, NY: 1991. p. 5-29.

Kerr JFR, Wyllie AH, Currie AR. Apoptosis: a basic biological phenomenon with wide-ranging implications in tissue kinetics. Br J Cancer 1972;26:239–257. [PubMed: 4561027]

Kinoshita JH, Merola LO. Hydration of the lens during the development of galactose cataract. Invest Ophthalmol 1964;47:577–584. [PubMed: 14238870]

Kinoshita JH, Kador P, Catiles M. Aldose reductase in diabetic cataract. J Am Med Assoc 1981;246:257–261.

Kosinski-Collins M, King J. *In vitro* unfolding, refolding, and polymerization of human γ-crystallin, a protein involved in cataract formation. Protein Sci 2003;12:480–490. [PubMed: 12592018]

Kumari SS, Varadaraj K, Valiunas V, Ramanan SV, Christensen EA, Beyer EC, Brink PR. Functional expression and biophysical properties of polymorphic variants of the human gap junction protein connexin 37. Biochem Biophys Res Commun 2000;274:216–224. [PubMed: 10903921]

Kumari SS, Varadaraj K, Valiunas V, Brink PR. Site-directed mutations in the transmembrane domain M3 of human connexin37 alter channel conductance and gating. Biochem Biophys Res Commun 2001;280:440–447. [PubMed: 11162536]

Kushmerick C, Rice SJ, Baldo GJ, Haspel HC, Mathias RT. Ion, water and neutral solute transport in Xenopus oocytes expressing frog lens MIP. Exp Eye Res 1995;61:351–362. [PubMed: 7556498]

Kuwahara M, Shinbo I, Sato K, Terada Y, Marumo F, Sasaki S. Transmembrane Helix 5 Is Critical for the High Water Permeability of Aquaporin. Biochemistry 1999;38:16340–16346. [PubMed: 10587459]

Kuwahara M, Iwai K, Ooeda T, Igarashi T, Ogawa E, Katsushima Y, Shinbo I, Uchida S, Terada Y, Arthus MF, Lonergan M, Fujiwara TM, Bichet DG, Marumo F, Sasaki S. Three families with autosomal dominant nephrogenic diabetes insipidus caused by aquaporin-2 mutations in the C-terminus. Am J Hum Genet 2001;69:738–748. [PubMed: 11536078]

La Porta CA, Gena P, Gritti A, Fascio U, Svelto M, Calamita G. Adult murine CNS stem cells express aquaporin channels. Biol Cell 2006;98:89–94. [PubMed: 15907198]

Lindsey Rose KM, Wang Z, Magrath GN, Hazard ES, Hildebrandt JD, Schey KL. Aquaporin 0-Calmodulin interaction and the effect of AQP0 phosphorylation. Biochemistry 2008;47:339–347. [PubMed: 18081321]

Liu CY, Kaufman RJ. The unfolded protein response. J Cell Sci 2003;116:1861–1862. [PubMed: 12692187]

Lomas DA, Carrell RW. Serpinopathies and the conformational dementias. Nat Rev Genet 2002;3:759–768. [PubMed: 12360234]

Mathias RT, Rae JL, Baldo GJ. Physiological properties of the normal lens. Phys Rev 1997;77:21–50.

Mathias RT, Kistler J, Donaldson P. The lens circulation. J Membr Biol 2007;216:1–16. [PubMed: 17568975]

Ma T, Yang B, Gillespie A, Carlson EJ, Epstein CJ, Verkman AS. Severely impaired urinary concentrating ability in transgenic mice lacking aquaporin-1 water channels. J Biol Chem 1998;273:4296–4309. [PubMed: 9468475]

Manley DM, McComb ME, Perreault H, Donald LJ, Duckworth HW, O'Neil JD. Secondary structure and oligomerization of the *E. coli* glycerol transporter. Biochemistry 2000;39:12303–12311. [PubMed: 11015209]

Mathai JC, Agre P. Hourglass Pore-Forming Domains Restrict Aquaporin-1 Tetramer Assembly. Biochemistry 1999;38:923–928. [PubMed: 9893987]

Marr N, Bichet DG, Lonergan M, Arthus MF, Jeck N, Seyberth HW, Rosenthal W, van Os CH, Oksche A, Deen PMT. Heteroligomerization of an aquaporin-2 mutant with wild-type Aquaporin- 2 and their misrouting to late endosomes/lysosomes explains dominant nephrogenic diabetes insipidus. Hum Mol Genet 2002;11:779–789. [PubMed: 11929850]

Mulders SM, Preston GM, Deen PMT, Guggino WB, Vanos CH, Agre P. Water channel properties of major intrinsic protein of lens. J Biol Chem 1995;270:9010–9016. [PubMed: 7536742]

Murata K, Mitsuoka K, Hirai T, Walz T, Agre P, Heymann JB, Engel A, Fujiyoshi Y. Structural determinants of water permeation through aquaporin-1. Nature 2000;407:599–605. [PubMed: 11034202]

Nemeth-Cahalan KL, Hall JE. pH and calcium regulate the water permeability of aquaporin 0. J Biol Chem 2000;275:6777–6782. [PubMed: 10702234]

Okamura T, Miyoshi I, Takahashi K, Mototani Y, Ishigaki S, Kon Y, Kasai N. Bilateral congenital cataracts result from a gain-of-function mutation in the gene for aquaporin-0 in mice. Genomics 2003;81:361–368. [PubMed: 12676560]

Patil RV, Saito I, Yang X, Wax MB. Expression of aquaporins in the rat ocular tissue. Exp Eye Res 1997;64:203–209. [PubMed: 9176054]

Pisano MM, Chepelinsky AB. Genomic cloning, complete nucleotide sequence, and structure of the human gene encoding the major intrinsic protein MIP of the lens. Genomics 1991;11:981–990. [PubMed: 1840563]

Pitonzo D, Skach WR. Molecular mechanisms of aquaporin biogenesis by the endoplasmic reticulum Sec61 translocon. Biochim Biophys Acta 2006;1758:976–988. [PubMed: 16782047]

Preston GM, Carroll TP, Guggino WB, Agre P. Appearance of water channels in Xenopus oocytes expressing red-cell CHIP28 protein. Science 1992;256:385–387. [PubMed: 1373524]

Preston GM, Jung JS, Guggino WB, Agre P. The mercury-sensitive residue at cysteine 189 in the CHIP28 water channel. J Biol Chem 1993;268:17–20. [PubMed: 7677994]

Preston GM, Smith BL, Zeidel ML, Moulds JJ, Agre P. Mutations in aquaporin-1 in phenotypically normal humans without functional chip water channels. Science 1994;265:1585–1587. [PubMed: 7521540]

Raman B, Rao CM. Chaperone-like activity and quaternary structure of alpha-crystallin. J Biol Chem 1994;269:27264–27268. [PubMed: 7961635]

Ren G, Cheng A, Melnyk P, Mitra AK. Visualization of a water-selective pore by electron crystallography in vitreous ice. J Struct Biol 2000;130:45–53. [PubMed: 10806090]

Robben JH, Knoers NV, Deen PM. Cell biological aspects of the vasopressin type-2 receptor and aquaporin 2 water channel in nephrogenic diabetes insipidus. Am J Physiol Renal Physiol 2006;291:F257–F270. [PubMed: 16825342]

Roudier N, Bailly P, Gane P, Lucien N, Gobin R, Cartron JP, Ripoche P. Erythroid expression and oligomeric state of the AQP3 protein. J Biol Chem 2002;277:7664–7669. [PubMed: 11751877]

Ruiz-Ederra J, Verkman AS. Accelerated cataract formation and reduced lens epithelial water permeability in aquaporin-1-deficient mice. Invest Ophthalmol Vis Sci 2006;47:3960–3967. [PubMed: 16936111]

Sandilands A, Hutcheson AM, Long HA, Prescott AR, Vrensen G, Loster J, Klopp N, Lutz RB, Graw J, Masaki S, Dobson CM, MacPhee CE, Quinlan RA. Altered aggregation properties of mutant γ-crystallins cause inherited cataract. EMBO J 2002;21:6005–6014. [PubMed: 12426373]

Schwartz LM, Smith SW, Jones MEE, Osborne BA. Do all programmed cell deaths occur via apoptosis? Proc Natl Acad Sci USA 1993;90:980–984. [PubMed: 8430112]

Shepshelovich J, Goldstein-Magal L, Globerson A, Yen PM, Rotman-Pikielny P, Hirschberg K. Protein synthesis inhibitors and the chemical chaperone TMAO reverse endoplasmic reticulum perturbation induced by over expression of the iodide transporter pendrin. J Cell Sci 2005;118:1577–1586. [PubMed: 15784681]

Shiels A, Bassnett S. Mutations in the founder of the MIP gene family underlie cataract development in the mouse. Nat Genet 1996;12:212–215. [PubMed: 8563764]

Shiels A, Mackay D, Bassnett S, Al-Ghoul K, Kuszak J. Disruption of lens fiber cell architecture in mice expressing a chimeric AQP0-LTR protein. FASEB J 2000;14:2207–2212. [PubMed: 11053241]

Shiels A, Bassnett S, Varadaraj K, Mathias R, Al-Ghoul K, Kuszak J, Donoviel D, Lilleberg S, Friedrich G, Zambrowicz B. Optical dysfunction of the crystalline lens in aquaporin-0-deficient mice. Physiol Genomics 2001;7:179–186. [PubMed: 11773604]

Sidjanin DJ, Parker-Wilson DM, Neuhauser-Klaus A, Pretsch W, Favor J, Deen PM, Ohtaka-Maruyama C, Lu Y, Bragin A, Skach WR, Chepelinsky AB, Grimes PA, Stambolian DE. A 76-bp deletion in the MIP gene causes autosomal dominant cataract in *Hfi* mice. Genomics 2001;74:313–319. [PubMed: 11414759]

Spector A. Oxidative stress-induced cataract: mechanism of action. FASEB J 1995;9:1173–1182. [PubMed: 7672510]

Stefani M, Dobson CM. Protein aggregation and aggregate toxicity: new insights into protein folding, misfolding diseases and biological evolution. J Mol Med 2003;81:678–699. [PubMed: 12942175]

Sui H, Han BG, Lee JK, Walian P, Jap BK. Structural basis of waterspecific transport through the AQP1 water channel. Nature 2001;414:872–878. [PubMed: 11780053]

Swamy-Mruthinti S. Expression and characterization of lens membrane intrinsic protein, MIP, in a baculovirus expression system. Curr Eye Res 1998;17:88–94. [PubMed: 9472476]

Swamy-Mruthinti S. Glycation decreases calmodulin binding to lens transmembrane protein, MIP. Biochim Biophys Acta 2001;1536:64–72. [PubMed: 11335105]

Swamy-Mruthinti S, Schey KL, Varadaraj K, Mathias RT. Decreased water permeability in diabetic rat lenses: Possible role of post-translational modifications of MIP Invest. Ophthalmol Vis Sci 1999;4ARVO Abstract, 4651

Tamarappoo BK, Verkman AS. Defective aquaporin-2 trafficking in nephrogenic diabetes insipidus and correction by chemical chaperones. J Clin Invest 1998;101:2257–2267. [PubMed: 9593782]

Trokel S. The physical basis for transparency of the crystalline lens. Invest Ophthalmol 1962;1:493–501. [PubMed: 13922578]

van Hoek AN, Wiener MC, Verbavatz JM, Brown D, Lipniunas PH, Townsend RR, Verkman AS. Purification and structure-function analysis of native, PNGase F-treated, and endo- -galactosidase-treated CHIP28 water channels. Biochemistry 1995;34:2212–2219. [PubMed: 7532004]

Varadaraj K, Skinner DM. Denaturants or cosolvents improve the specificity of PCR amplification of a G+C-rich DNA using genetically-engineered DNA-polymerases. Gene 1994;140:1–5. [PubMed: 8125324]

Varadaraj K, Kumari SS, Skinner DM. Actin-encoding cDNAs and gene expression during the intermolt cycle of the Bermuda land crab *Gecarcinus lateralis*. Gene 1996;171:177–184. [PubMed: 8666269]

Varadaraj K, Kumari SS, Skinner DM. Molecular characterization of four members of the alpha-tubulin gene family of the Bermuda land crab *Gecarcinus lateralis*. J Exp Zool 1997;278:63–77. [PubMed: 9143139]

Varadaraj K, Kushmerick C, Baldo GJ, Bassnett S, Shiels A, Mathias RT. The role of MIP in lens fiber cell membrane transport. J Membr Biol 1999;170:191–203. [PubMed: 10441663]

Varadaraj K, Kumari SS, Mathias RT. Lens major intrinsic protein vesicle trafficking requires a sorting signal. Invest Ophthalmol Vis Sci 2000;41ARVO Abstract, 4591

Varadaraj K, Kumari S, Shiels A, Mathias RT. Regulation of aquaporin water permeability in the lens. Invest Ophthalmol Vis Sci 2005;46:1393–1402. [PubMed: 15790907]

Varadaraj K, Kumari S, Mathias RT. Functional expression of aquaporins in embryonic, postnatal, and adult mouse lenses. Dev Dyn 2007;236:1319–1328. [PubMed: 17377981]

Verbavatz JM, Brown D, Sabolic I, Valenti G, Ausiello DA, van Hoek AN, Ma T, Verkman AS. Tetrameric assembly of CHIP28 water channels in liposomes and cell membranes. A freeze-fracture study. J Cell Biol 1993;123:605–618. [PubMed: 7693713]

Verkman AS. Role of aquaporin water channels in eye function. Exp Eye Res 2003;76:137–143. [PubMed: 12565800]

Walz T, Hirai T, Murata K, Heymann JB, Mitsuoka K, Fujiyoshi Y, Smith BL, Agre P, Engel A. The three-dimensional structure of aquaporin-1. Nature 1997;387:624–627. [PubMed: 9177353]

Willis D, Foglesong D, Granoff A. Nucleotide sequence of an immediate-early frog virus 3 gene. J Virol 1984;52:905–912. [PubMed: 6092719]

Wistow GJ, Pisano MM, Chepelinsky AB. Tandem sequence repeats in transmembrane channel proteins. Trends Biochem Sci 1991;16:170–171. [PubMed: 1715617]

Zampighi GA, Kreman M, Boorer KJ, Loo DD, Bezanilla F, Chandy G, Hall JE, Wright EM. A method for determining the unitary functional capacity of cloned channels and transporters expressed in *Xenopus laevis* oocytes. J Membr Biol 1995;148:65–78. [PubMed: 8558603]

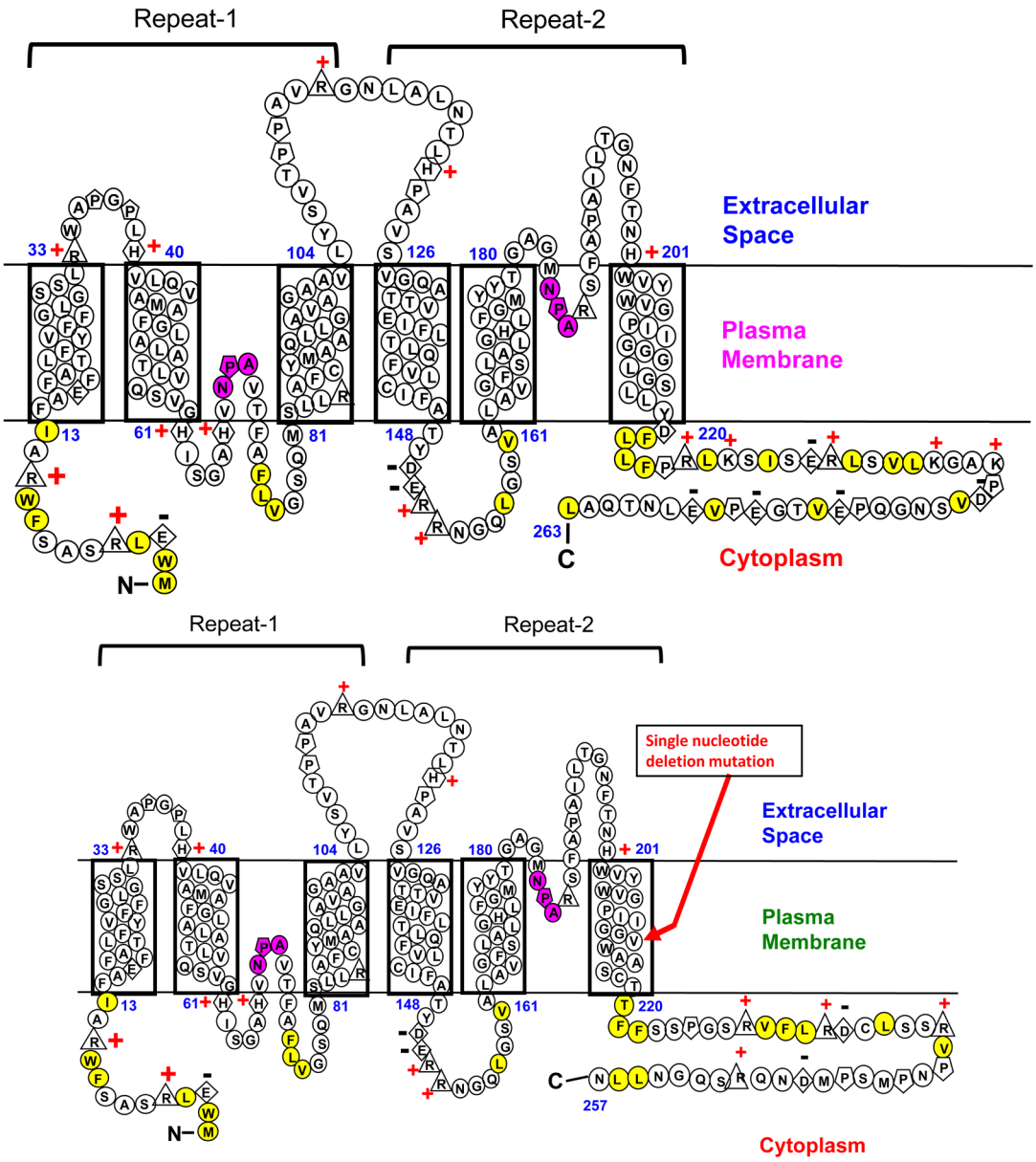

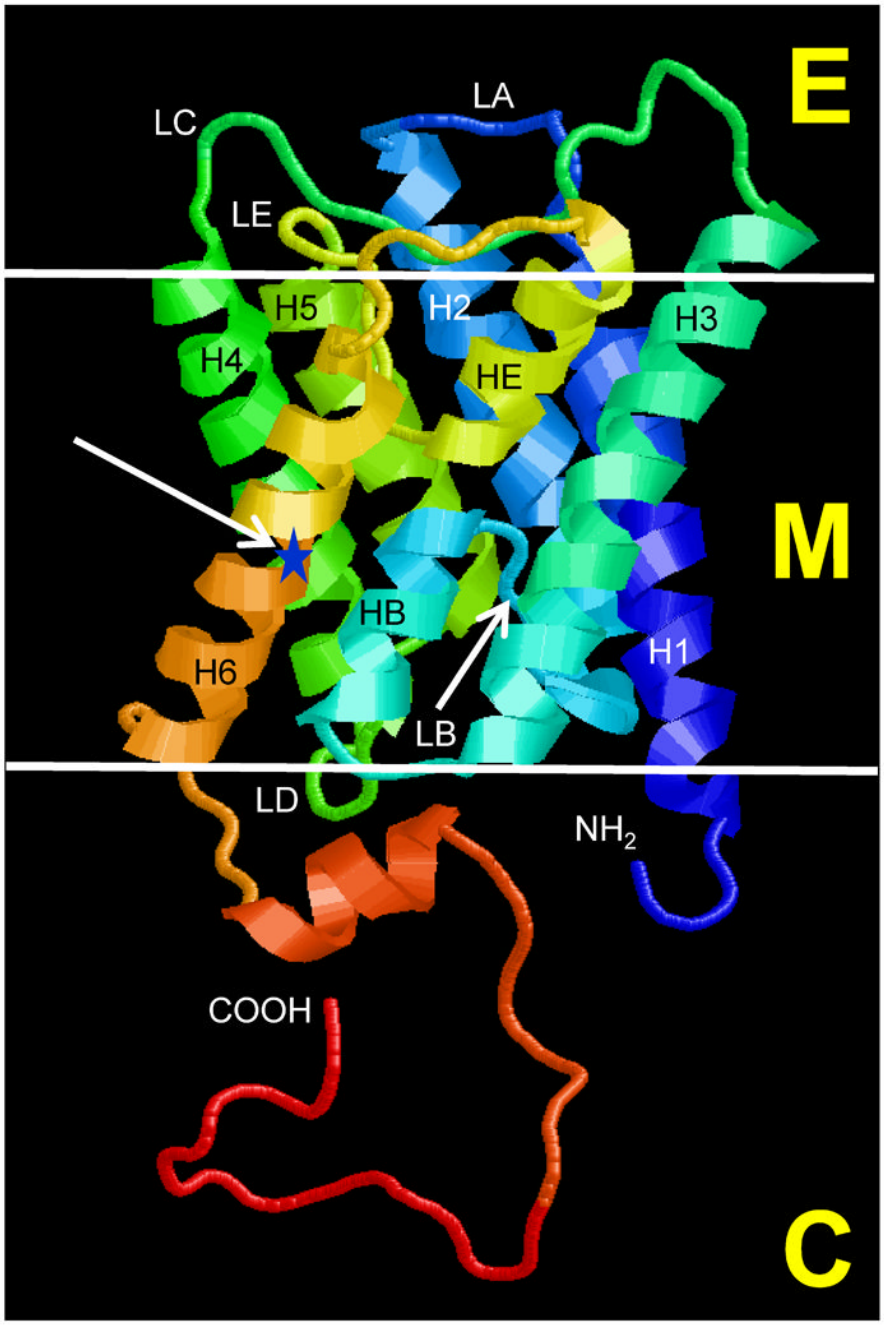

Fig. 1.

Schematic representations. (A) Human WT-AQP0 and (B) Δ213-AQP0. Yellow circles represent hydrophobic amino acids in the cytoplasmic domains and '+' and '−' represent amino acid charges in the extracellular and cytoplasmic domains. (C), 3-D model of wild type human AQP0 protein predicted using 3D-JIGSAW (version 2.0). The monomer is rendered in cartoon. Monomeric structure shows folds, helix assignment, and location in the membrane. Membrane-spanning helices are denoted as LH1–LH6 and loops as LA–LE. The two pore lining helices are shown as HB and HE. Site of the mutation and frameshift is represented with a blue star (indicated by a red arrow). E, extracellular space; M, membrane; C, cytoplasm, NH2, amino terminus; COOH, carboxy terminus.

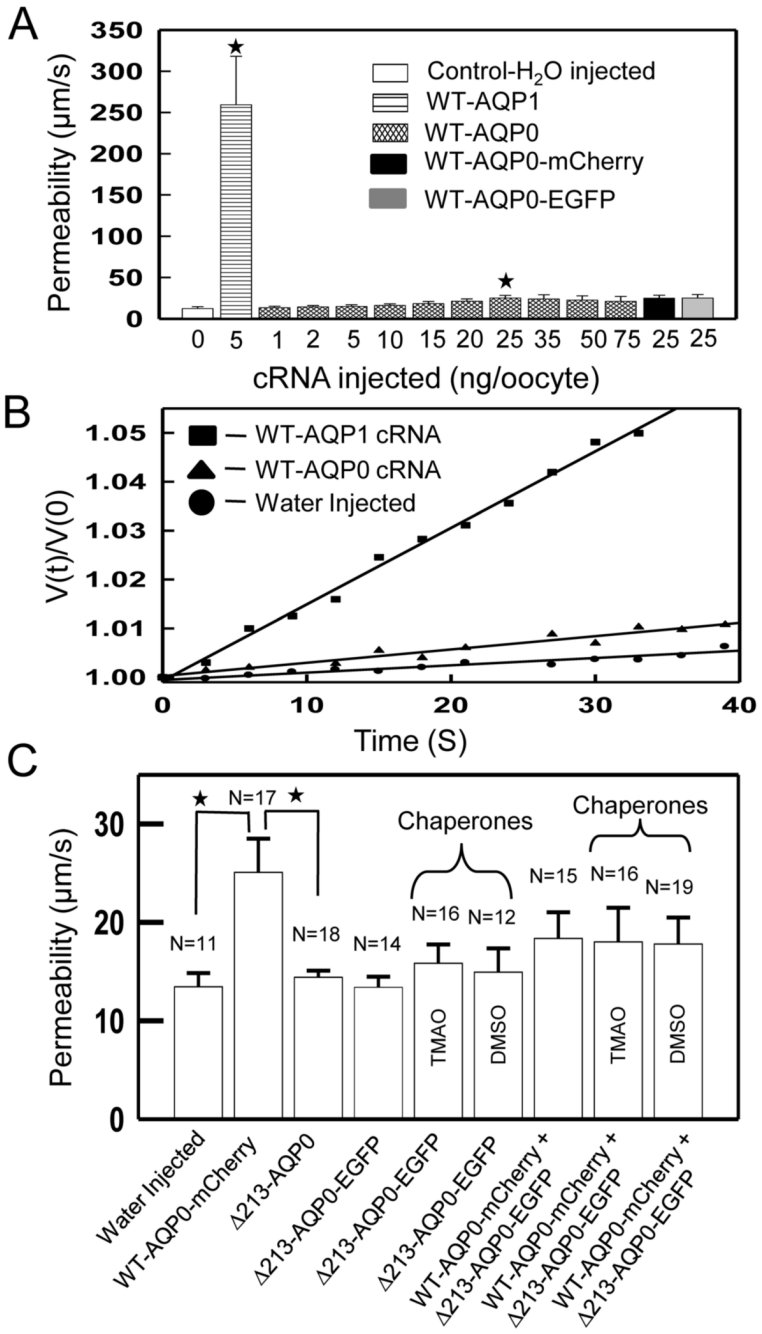

Fig. 2.

Water permeability of WT-AQP0 and Δ213-AQP0. (A) Membrane water permeability of *Xenopus laevis* oocytes injected with (from left to right): distilled water; 5 ng/oocyte cRNA for WT-AQP1; 1, 2, 5, 10, 15, 20, 25, 35, 50, or 75 ng/oocyte cRNA for WT-AQP0; 25 ng/oocyte cRNA for WT-AQP0-mCherry; 25 ng/oocyte cRNA for WT-AQP0-EGFP. Membrane water permeability was determined using the oocyte swelling assay as described in the 'Materials and Methods' section. Oocyte membrane water permeability of five swelling assays (each assay with 10 oocytes; (mean ± SD)) is shown. (B) Representative data on *X. laevis* oocytes injected with distilled water, cRNA for human AQP1 or cRNA for human AQP0. An oocyte was placed in a hypotonic solution and the initial rate of swelling was estimated. A

simple curve fit to the data was obtained to calculate the oocyte membrane water permeability as described in 'Materials and Methods' section. Relative water uptake for distilled water injected control, human AQP1-cRNA or human AQP0-cRNA expressing oocyte is given. (C) Membrane water permeability of *X. laevis* oocytes injected with (from left to right): distilled water; 25 ng of cRNA for WT-AQP0-mCherry; 25 ng of cRNA for Δ213-AQP0; 25 ng of cRNA for Δ213-AQP0-EGFP; 25ng/oocyte cRNA for WT-AQP0-mCherry + 25ng/oocyte cRNA for Δ213-AQP0-EGFP. In some experiments, we have incubated the cRNA injected oocytes in the chemical chaperones TMAO (100 mM) or DMSO (0.5%). Each bar represents the mean ± SD from five swelling assays. N, number of oocytes used per experiment. Asterisk represents the degree of significance in comparison with control, $P < 0.0001$.

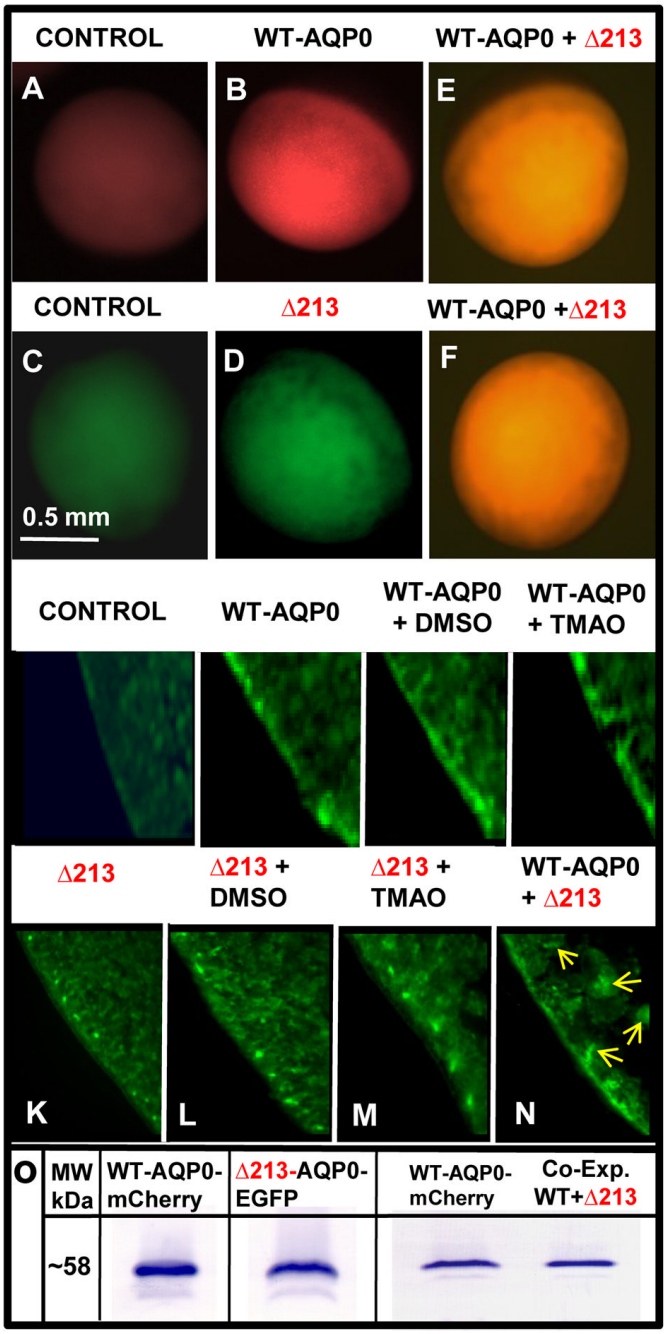

Fig. 3.

Expression of WT-AQP0 and Δ213-AQP0 in the *X. laevis* oocytes. (A–F) Epifluorescence of *X. laevis* oocyte injected with distilled water or AQP0 cRNAs, (A,C) Oocytes injected with distilled water, (B) Oocyte injected with WT-AQP0-mCherry cRNA, (D) Oocyte injected with Δ213-AQP0-EGFP cRNA, (E,F) Oocytes co-injected with WT-AQP0-mCherry and Δ213-AQP0-EGFP cRNAs. (G–N) Immunostaining of cryosections of oocytes injected with distilled water or AQP0 cRNAs. Expression of WT-AQP0 was visualized by immunostaining using anti-AQP0 antibody. Since the antibody was raised against 17 amino acids from the C-terminal domain, it did not bind to Δ213-AQP0 protein. Therefore, EGFP fluorescence was used to visualize the localization of the mutant protein. (G) Water injected oocyte. The other oocytes

shown were injected with cRNA for: WT-AQP0-mCherry (H), WT-AQP0-mCherry and incubated in 0.5% DMSO (I), WT-AQP0-mCherry and incubated in 100 mM TMAO (J), Δ213-AQP0-EGFP (K), Δ213-AQP0-EGFP and incubated in 0.5% DMSO (L), Δ213-AQP0-EGFP and incubated in100mM TMAO (M), WT-AQP0 + Δ213-AQP0 and immunostained for WT (N). As shown in N, when WT- and Δ213-AQP0 without any fluorescent tag are co-expressed, even though some WT appeared to get to the plasma membrane, there was significant subcellular accumulation (arrows). (O) Western blot analysis of oocytes injected with cRNAs of WT-AQP0-mCherry (lanes 1 and 3), Δ213-AQP0-EGFP (lane 2), and WT-AQP0-mCherry + Δ213-AQP0-EGFP (lane 4).

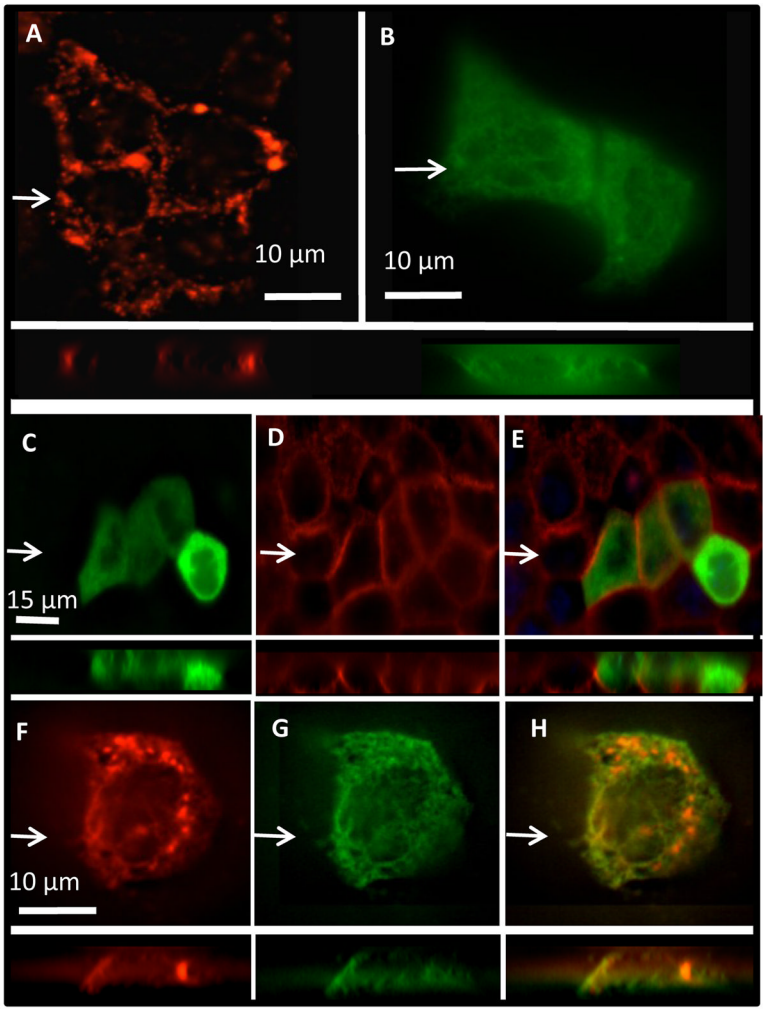

Fig. 4.

Localization and co-localization of WT-AQP0-mCherry or/and Δ213-AQP0-EGFP in transfected MDCK cells. (A, B) Epifluorescent images of cells transfected with the WT-AQP0-mCherry and Δ213-AQP0-EGFP, respectively. (C–E) To confirm the plasma membrane localization of Δ213-AQP0-EGFP, cells were fixed and incubated with Texas Red-conjugated wheat germ agglutinin without permeabilization to label glycoproteins in the plasma membrane; (C) cell viewed under EGFP fluorescent filter for Δ213-AQP0-EGFP expression; (D) the same cell under an Texas Red fluorescent filter for plasma membrane staining; (E) overlaid image of (C) and (D). (F–H) A cell co-transfected with Δ213-AQP0-EGFP and WT-AQP0-mCherry constructs; (F) co-transfected cell viewed under mCherry fluorescent filter; (G) the same cell under an EGFP fluorescent filter; (H) overlaid image of (F) and (G). For A–H, confocal images were taken in the xy-axis (top) and xz-axis (bottom); white arrows indicate the position of the XZ axis).

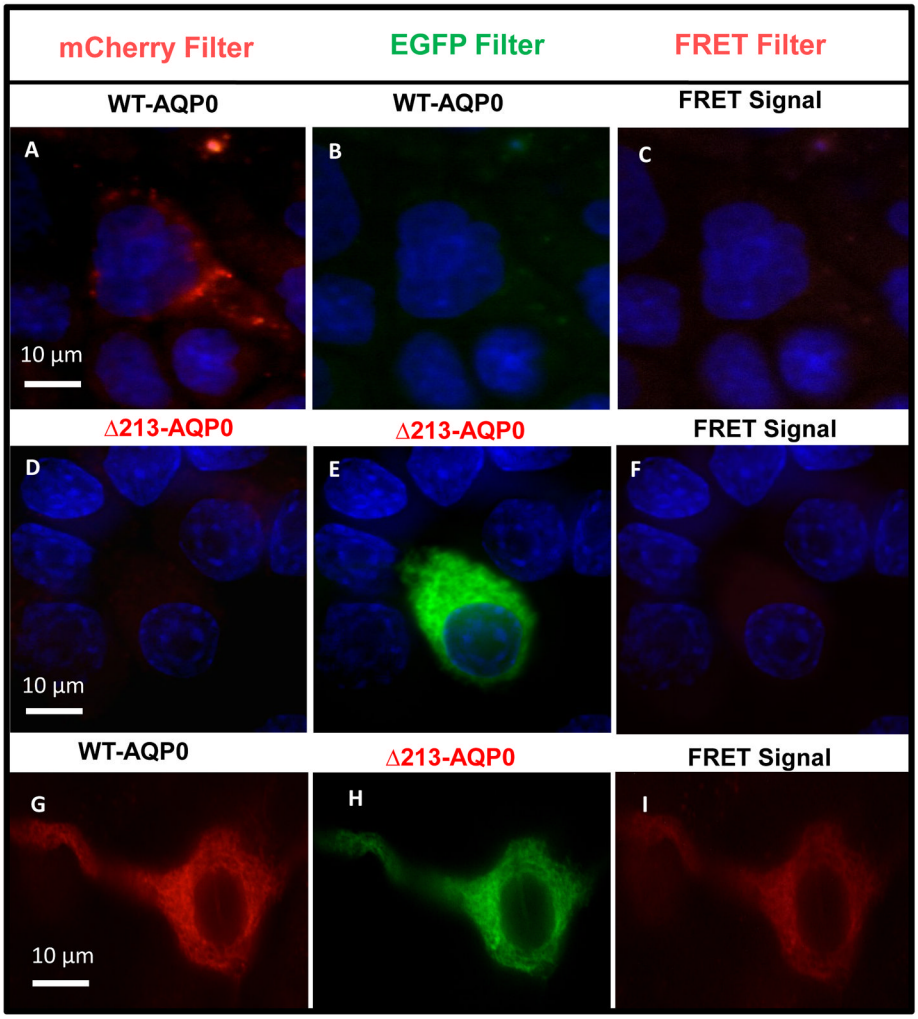

Fig. 5.

Co-localization of WT-AQP0-mCherry and Δ213-AQP0-EGFP in transfected cells. (A–I) Forster Resonance Energy Transfer in an N2A or MDCK cells transfected with WT-AQP0-mCherry or/and Δ213-AQP0-EGFP. Cells were transfected with only WT-AQP0-mCherry (A-C) or Δ213-AQP0-EGFP (D–F) as controls to monitor background fluorescence; (A, D, G) cells excited at 587 nm and emission recorded at 610 nm; (B, E, H) cells excited at 488 nm and emission recorded at 507 nm; (C, F, I) fluorescence due to FRET; (I) fluorescence indicating co-localization of WT-AQP0-mCherry and Δ213-AQP0-EGFP proteins in the same oligomer or within 100Å.

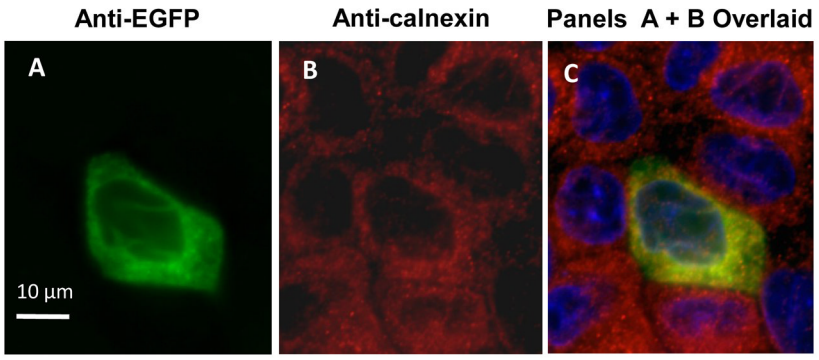

Fig. 6.

Co-localization of ER-resident protein and Δ213-AQP0-EGFP in transfected MDCK cells. (A-C) MDCK cells expressing Δ213-AQP0-EGFP immunostained for native ER protein, calnexin, and detected using Texas Red conjugated secondary IgG. (A) Cells viewed under EGFP fluorescent filter; (B) same cells viewed under Texas Red fluorescent filter; (C) overlaid images of (A) and (B).

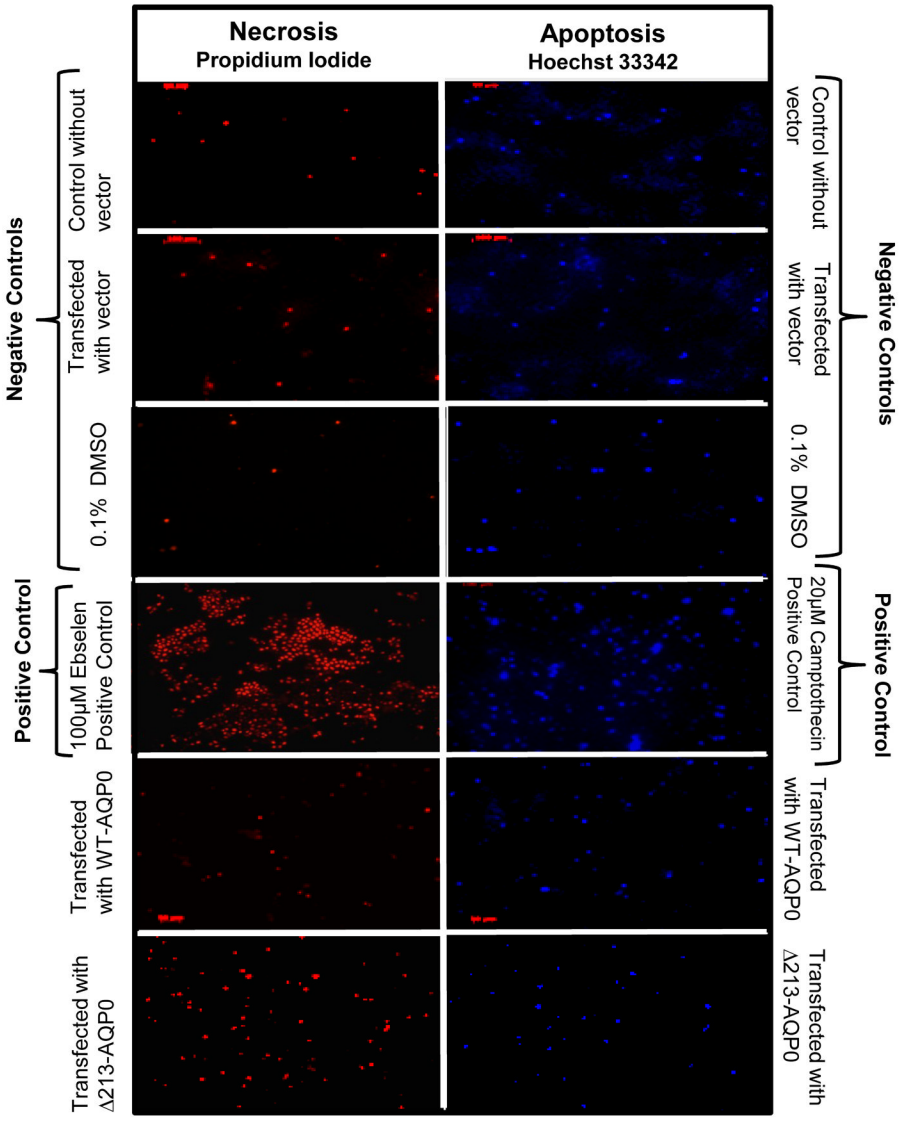

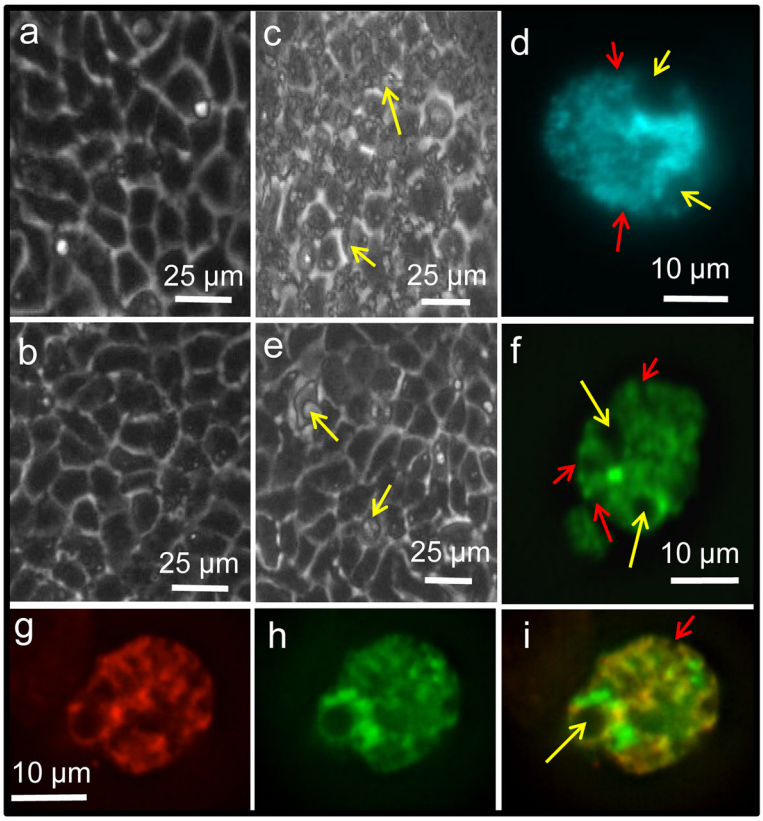

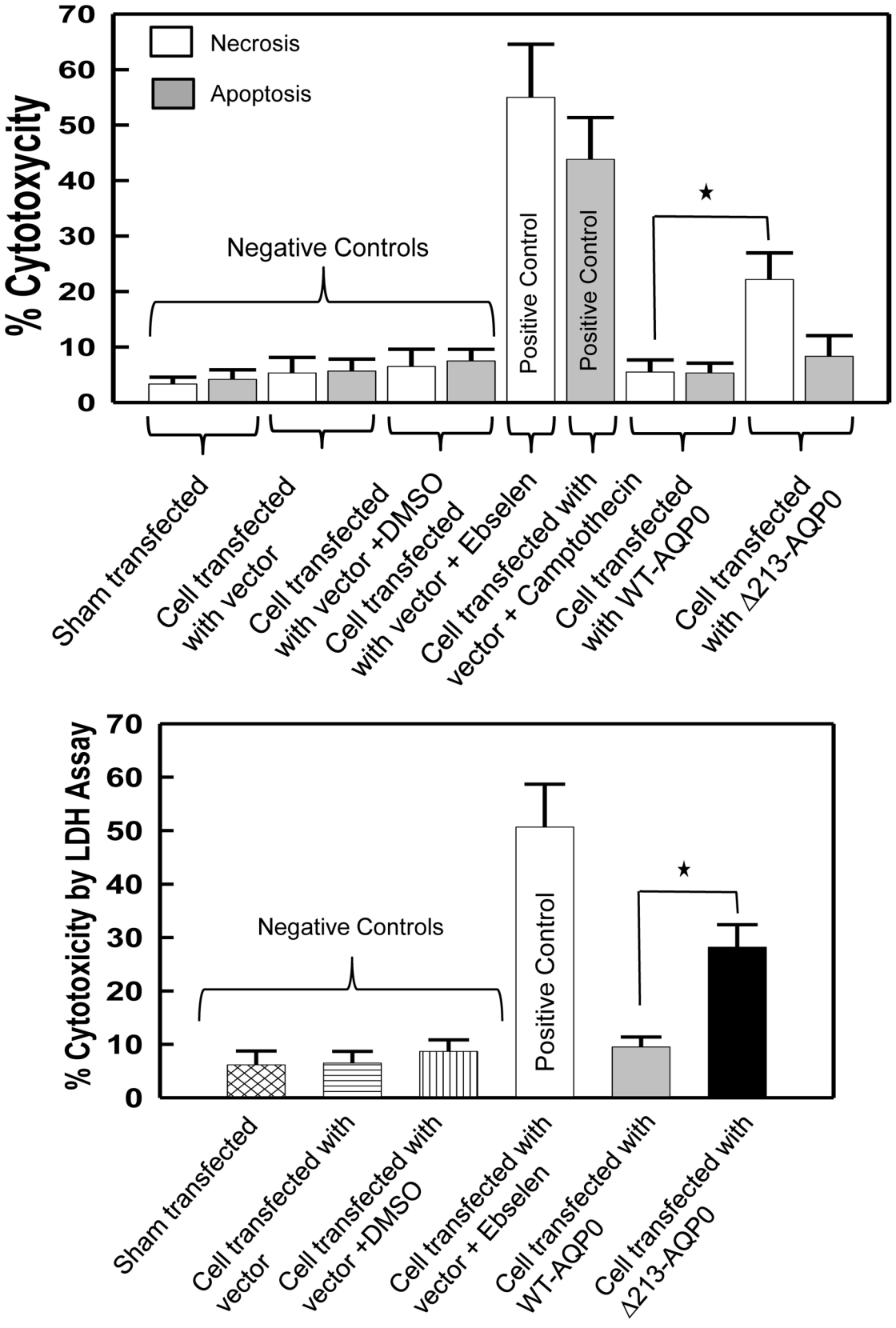

Fig. 7.

Morphological and Biochemical assessments of cytotoxicity due to Δ213-AQP0. (A) Necrosis and apoptosis in MDCK cells transfected with WT-AQP0 or Δ213-AQP0. Propidium iodide (bright red) staining for necrosis and Hoechst 33342 (bright blue), staining for apoptosis. Ebselen (100 μM) and camptothecin (20 μM) were used as positive controls for necrosis and apoptosis, respectively. Panel B: Sham transfected MDCK cells (a) showing cuboidal shape; MDCK cells transfected with WT-AQP0 (b) showing similar morphology as sham transfected cells; MDCK cells treated with ebselen (c) showing characteristics of necrosis; magnified view of an MDCK cell (pseudocolored) treated with ebselen (d) showing vacuoles (yellow arrows) and membrane breakage (red arrows); MDCK cells transfected with Δ213-AQP0 (e); several cells showed vacuoles similar to ebselen treated necrotic cells (yellow arrows); magnified view of an MDCK cell expressing (pseudocolored) Δ213-AQP0 (f) showing vacuoles (yellow arrow) and membrane breakage (red arrows); (g–i) a necrotic cell; (g) co-transfected (WT-AQP0-mCherry and Δ213-AQP0-EGFP) cell viewed under mCherry fluorescent filter; (h) the same cell viewed under an EGFP fluorescent filter; (i) overlaid image of (g) and (h). (C) Quantification of necrosis or apoptosis in percentage over healthy cells. (D) Percentage cytotoxicity due to Δ213-AQP0 protein calculated using a colorimetric assay which measures lactate dehydrogenase (LDH) activity. Results are shown in percentage of total cellular LDH release due to cellular membrane damage. Results are represented by the mean from triplicate of five independent assays; *error bars* represent standard deviation of the mean. Asterisk represents the degree of significance in comparison with control, $P<0.0001$.

Table 1

Partial nucleotide and amino acid sequences of human wild type and Δ213-AQP0; *-stop codon; the red arrow shows the single nucleotide base deletion mutation which resulted in a frameshift and yielded a short mutant protein of 257 amino acids rather than 263 amino acid in the wild type; 90% of the amino acids at the proximal region of the intracellular C-terminal domain are different compared to the wild type.